ANKARA YILDIRIM BEYAZIT UNIVERSITY

GRADUATE SCHOOL OF NATURAL AND APPLIED SCIENCES

PRODUCTION OF GRADIENT POROUS SILICON NITRIDE CERAMICS FOR BONE GRAFTING APPLICATIONS

M.Sc. Thesis by

Serdar Onat AKBULUT

Department of Materials Engineering

January, 2020

ANKARA

PRODUCTION OF GRADIENT POROUS SILICON NITRIDE CERAMICS FOR BONE GRAFTING APPLICATIONS

A Thesis submitted to

The Graduate School of Natural and Applied Sciences of

Ankara Yildirim Beyazit University

In Partial Fulfillment of the Requirements for the Degree of Master of Science

in Materials Engineering, Department of Materials Engineering

by

Serdar Onat AKBULUT

January, 2020

ANKARA

M.Sc. THESIS EXAMINATION RESULT FORM

We have read the thesis entitled with **"PRODUCTION OF GRADIENT POROUS SILICON NITRIDE CERAMICS FOR BONE GRAFTING APPLICATIONS"** completed by **SERDAR ONAT AKBULUT** under supervision of **Assist. Prof. Dr. GÜLSÜM TOPATEŞ** and we certify that in our opinion it is fully adequate, in scope and in quality, as a thesis for the degree of Master of Science.

Assist. Prof. Dr. Gülsüm TOPATEŞ

Supervisor

Prof. Dr. Leyla Didem KOZACI

Jury Member

Prof. Dr. H. Canan CABBAR

Jury Member

Prof. Dr. Cihangir DURAN

Jury Member

Prof. Dr. Ergün ERARSLAN

Director
Graduate School of Natural and Applied Sciences

ETHICAL DECLERATION

I hereby declare that, in this thesis has been prepared in accordance with the Thesis Writing Manual of Graduate School of Natural and Applied Sciences,

- All data, information and documents are obtained in the framework of academic and ethical rules,
- All information, documents and assessments are presented in accordance with scientific ethics and morals,
- All the materials that have been utilized are fully cited and referenced,
- No change has been made on the utilized materials,
- All the works presented are original,

and in any contrary case of above statements, I accept to renounce all my legal rights.

Date: 14.01.2020 **Signature:**

Name & Surname: Serdar Onat AKBULUT

ACKNOWLEDGMENTS

I would like to show my appreciation to my supervisor Assist. Prof. Dr. Gülsüm TOPATEŞ for her patience, valuable guidance, supports and advices. I would like to express my gratitude to all those who gave me the possibility to complete this thesis. I would like to thank to Prof. Dr. Leyla Didem KOZACI for the cell culture and other biocompatibility experiments and also her infinite support. I thank to Assoc. Prof. Dr. Erhan AYAS and Res. Assist. Kübra GÜRCAN for the sintering of the samples. I am very thankful to Res. Assist. Büşra GÖRGÜN, Kübra FİDAN and Gülben AKCAN for the biocompatibility analysis, their supports, patience and helps. Also, I thank to Assist. Dr. Betül ÖZBEK İPTEÇ for the teaching protocols of the cell culture to me.

I would like to express my gratefulness to my mother and father for their infinite support and deepest love.

I am also very thankful for Ankara Yildirim Beyazit University for the 5363 BAP project.

2020, 14 January **Serdar Onat AKBULUT**

PRODUCTION OF GRADIENT POROUS SILICON NITRIDE CERAMICS FOR BONE GRAFTING APPLICATIONS

ABSTRACT

The aim of this study is to produce gradient porous silicon nitride samples with the similar pore structure of bone. In this thesis, the tape casting method was chosen for the production of the gradient porous silicon nitride samples where the porous structure was obtained by addition of two different types pore formers (PVC and PMMA). Three types of tape slurries were prepared; two slurries from different pore formers and one slurry without pore former. Gradient structure prepared by lamination of three tapes. Laminated sample was kept in burn-out for removing polymeric substances and pore formers, then they were sintered under nitrogen atmosphere at 1700°C for 3 hours. Physical (density, porosity, etc.), phase and microstructural properties were characterized. A gradient pore structure successfully obtained according to SEM analysis, a gradual decrease in pore size was obtained along the cross-section of the samples. Also, mercury porosimetry analysis proved the formation of different pore sizes.

Cell culture test was done by using osteoblast-like cells. Cytotoxic and biocompatibility behaviors of the sample was evaluated by two methods which are responsible for cell proliferation (WST-1) and cytotoxicity (LDH). The cell proliferation increased and attachment of cells on the surface of the scaffolds was observed. Likewise, the samples did not show any cytotoxic evaluation due to LDH results. As a result, gradient porous silicon nitride samples are biocompatible and have a possibility to using as a bone substitute element.

Keywords: Gradient porosity, tape casting, silicon nitride, cytotoxicity, cell proliferation.

KEMİK GREFTİ KULLANIMI İÇİN AŞAMALI GÖZENEK YAPISINA SAHİP SİLİSYUM NİTRÜR SERAMİKLERİNİN ÜRETİMİ

ÖZ

Bu çalışmanın amacı kemiğin gözenek yapısına benzer, aşamalı gözeneğe sahip silisyum nitrür seramiklerinin üretilmesidir. Bu tez kapsamında aşamalı gözeneğe sahip silisyum nitrür seramiklerinin üretiminde şerit döküm tercih edilmiş olup, gözenekli yapısı, gözenek oluşturucu (PVC and PMMA) ilavesiyle elde edilmiştir. İki çamur gözenek oluşturucular için ve bir çamur gözenek oluşturucu ilavesiz olacak şekilde üç farklı çamur hazırlanmıştır. Aşamalı gözenek yapısı üç farklı şeridin laminasyonu ile elde edilmiştir. Lamine edilen numuneler polimer esaslı maddelerin ve gözenek oluşturucuların uzaklaştırılması için ısıl işleme tabii tutulmuş ve ardından azot atmosferi altında 1700°C'de 3 saat sinterlenmiştir. Fiziksel (yoğunluk, gözenek, vb.) mikroyapısal ve faz özellikleri analiz edilmiştir. Kesit alanının SEM analizi sonuçlarına göre aşamalı gözenek yapısı başarı ile elde edilmiştir. Bununla birlikte, civa porozimetresi analizi sonuçları farklı gözenek oluşumlarını kanıtlamıştır.

Hücre kültürü çalışmalarında osteoblast-benzeri hücreler kullanılmıştır. Numunelerin sitotoksik ve biyouyumluluk davranışları hücre çoğalması (WST-1) ve sitotoksik analiz (LDH) olmak üzere iki farklı yöntemle incelenmiştir. Sonuçlara bakıldığında numune yüzeyinde hücrelerin çoğaldığı gözlemlenmiştir. Aynı şekilde, LDH analizlerine bakıldığında numunelerin hücre üzerinde herhangi bir sitotoksik bulunmadığı görülmüştür. Sonuç olarak, aşamalı gözenekli silisyum nitrür seramikleri biyouyumludur ve kemik grefti olarak kullanım potansiyeline sahiptir.

Anahtar Kelimeler: Aşamalı gözenek, şerit döküm, silisyum nitrür, sitotoksisite, hücre çoğalması.

CONTENTS

ABBREVIATIONS

MPa	Mega Pascal
Al_2O_3	Aluminum Oxide
ZrO_2	Zirconium Oxide
CaO	Calcium Oxide
MgO	Magnesium Oxide
TiN	Titanium Nitrate
N_2	Nitrogen
$CaCO_3$	Calcium Carbonate
SiO_2	Silicon Oxide
Si	Silicon
O	Oxygen
Ca	Calcium
Y_2O_3	Yttria
Yb_2O_3	Yterbium Oxide
α-Si_3N_4	alpha-silicon nitride
β-Si_3N_4	beta-silicon nitride

Acronyms

TCP	Tricalcium phosphate
PU	Polyurethane
PS	Polystyrene
UF	Urea Formaldehyde
DBM	Demineralized Bone Matrix
PRP	Platelet Rich Plasma

CDG	Coral Derived Granules
HA	Hydroxyapatite
BMP	Bone Morphogenetic Proteins
IGF	Insulin-like Growth Factor
TGF	Transforming Growth Factor
FGF	Fibroblast Growth Factor
SEM	Scanning Electron Microscope
RBSN	Reaction Bonded Silicon Nitride
PMMA	Polymethylmethacrylade
XRD	X-Ray Diffraction
HMSC	Human Mesenchymal Stem Cells
CT	Computer Tomography
MR	Magnetic Resonance
PVC	Polyvinyl Chloride
TG-DTA	Thermogravymetric- Differential Thermal Analysis
EDX	Energy Dispersive X-Ray Spectroscopy
DMEM	Dulbecco's Modified Eagle Medium
FBS	Fetal Bovine Serum
GFP	Green Fluorescent Protein
ATP	Adenosine Triphosphate
LDH	Lactate Dehydrogenase
MTT	3-(4,5-dimethylthiazol-2-yl)-2,5-diphenyltetrazolium bromide
PES	Phenazine Ethosulfate
PMS	Phenazine Methosulfate
NAD	Nicotinamide Adenine Dinucleotite

DNA	Deoxyribonucleic acid
DAPI	4’,6-diamidino-2-phenylindole

NOMENCLATURE

nm	Nanometer
º	Degree
º C	Degree Celcius
wt. %	Percent in Weight
vol. %	Percent in Volume
ppm	Parts per Million
µm	Micronmeter
Sec.	Second
Min.	Minute
cm	Centimeter
g	Gram
mm	Millimeter
θ	Wetting Angle
γ	Surface Tension
d	Diameter
P	Pressure
A	Area

LIST OF TABLES

LIST OF FIGURES

CHAPTER 1

INTRODUCTION

1.1 Porous Ceramics and Production Methods

Porosity contained materials have very special characteristics that cannot be achieved by the conventional routes. Consequently, porous materials became final products for some potential applications such as polymer-based foams for packaging and for buildings and airplanes aluminum-based light-weight materials and for water purification systems ceramic based materials. In contrast to porous metallic and polymeric materials, porosity has been kept away from ceramic materials because of the brittleness of them. On the other hand, an increment on some potential applications created requirements such as high temperature, corrosive and wear media environment showed necessity to porous ceramics. Molten metal filtration, insulation applications for high temperature and corrosive gas filtration can be examples. The microstructure, type of porosity and pore size distribution are tailorable properties and they directly affect on the properties of the ceramics [1].

Porosity in biomaterials is broaden the area of usage. Several pore size and pore size distribution can be achieved, and hence gradient porosity can be obtained [2].

Examples of the porosity contained materials were given in Figure 1.1.

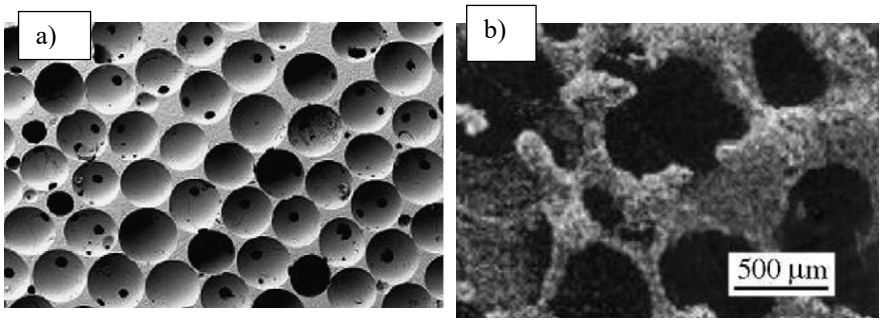

Figure 1.1 Examples of porous a) metal; (b) TCP for biomedical applications [3-4]

Porous metals and porous TCP which can be seen in Figure 1.1 are widely used in biomedical fields.

Porosity of ceramics in the meaning of size can be divided into three categories that are macroporous (d>50 nm), mesoporous (2 nm<d<50 nm) and microporous (d<2 nm). Mainly some methods that is used for preparation of cellular ceramics such as foams, honeycomb and interconnected rods have been researched [1-8].

Beside the conventional production methods for cellular ceramics some methods were also developed. These techniques are replica method, sacrificial template and direct foaming method.

Total porosity is very important parameter for all porous materials, but total porosity has negative effect on the mechanical properties. A porous material can have both open and closed pores at the same time. Connected pores are conductive for gaseous, liquids and particle included suspensions.

The schematic representation of pore characteristics was given in Figure 1.2.

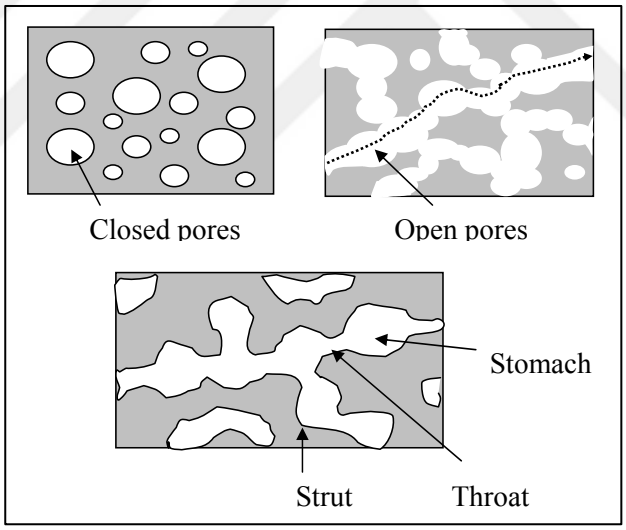

Figure 1.2 Illustration of the pore characteristics in the porous ceramics [2].

The open and closed porosity and strut, stomach and throat can be found in almost both open pores contained ceramics which were represented in Figure 1.2.
Except pore interconnectivity, pore size and pore size distribution have an importance. Micropores generally are found in the struts and they connect the macro-pores heterogeneously.

The porous ceramics can be fabricated in various techniques due to these techniques; pores can be obtained in various characteristics and sizes. Mainly, the macroporous ceramics can be fabricated with three methods that are replica technique, sacrificial template method and direct foaming method.

1.1.1 Replica Technique

In replica method, a synthetic or natural template can be used as replication substrate. In synthetic replica method, generally polymer based (especially polyurethane) highly porous sponges are used.

This ceramic suspension is impregnated to the sponge until all internal pores are filled completely with ceramic suspension. After sponge is coated by ceramic suspension, for removing of the excess slurry, is done by the roller to prevent formation of thinner coating on the struts. The slurry should have enough viscosity to avoid dripping. For efficiently coating of polymeric template, the slurry should show shear-thinning behavior and the shear-thinning can achieve by the usage of thixotropic and thickening additives. After coating, the polymer should be pyrolyzed with controlled heating process.

After successful completion of the pyrolysis step, the ceramic substrate can be sintered at suitable temperatures for densification. The disadvantage of this method is the struts on the reticulated structures can be cracked during removing of polymeric template and this issue reduces the mechanical properties. Moreover, the synthetic templates, natural templates have been used for the fabrication of the porous ceramics. Cellular templates in nature are very interesting templates because of their unique pore morphology and microstructure and producing of a material with these properties artificially can be difficult. Corals are well-known natural template to produce microporous ceramics especially for the tissue engineering and bone replacement.

The coral is impregnated to the wax under vacuum and negative form is obtained. Then, the ceramic slurry is impregnated to the wax, which is negative form of coral, after that the wax pyrolyzed.
The illustration of replica method was given in Figure 1.3.

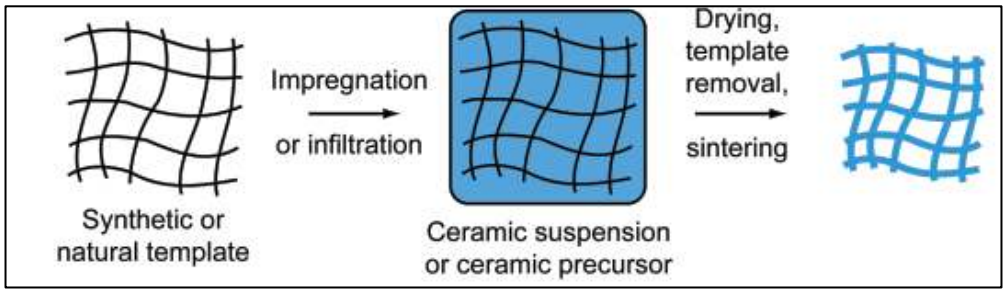

Figure 1.3 Impregnation of synthetic or natural template into the ceramic suspension or ceramic precursor [1].

1.1.2 Sacrificial Template Method

The second method for fabrication of the cellular ceramics is sacrificial template method. This technique includes two different phases, and sacrificial phases can be homogeneously distributed into ceramic precursor or continuous matrix of ceramic particles. The biphasic composite usually prepared with two methods that are pressing of the two components (powder mixture and pore forming agent), obtaining two-phase suspension with following wet colloidal routes which are tape, slip or direct casting methods, or impregnation of the preceramic polymer or ceramic suspension to consolidated preforms of the sacrificial template.

Wide variety of pore formers even natural or synthetic such as salts, metals, liquids, etc. can be used and they pyrolyzed under long thermal treatment at temperatures between 200^{o} and 600^{o}C. This long period heat treatment causes gas releases at extensive amounts from the pore forming agents which is main disadvantage of the using sacrificial phase.

However, sacrificial template method is almost suitable to several chemical compositions for fabrication processes.

Advantageously, in sacrificial template method, tailoring the porosity, pore size distribution and pore morphology of the final ceramic product is more controllable than other techniques.

The sacrificial phase does not allow the flaws in the struts which means that the mechanical strength is relatively higher than the other techniques to fabrication of porous materials. In macro-porous ceramics produced with sacrificial template method, the strength depends on the open and closed pores.

The route of sacrificial template method for the production of porous ceramic is illustrated in Figure 1.4.

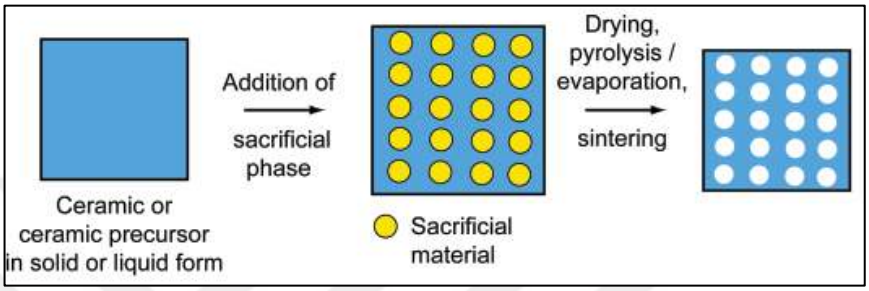

Figure 1.4 Addition of sacrificial phase into the ceramic suspension [1].

1.1.3 Direct Foaming Method

The third method is direct foaming method, where the porous ceramics are fabricated by addition of air or liquid media into ceramic precursor. The amount of total porosity directly depends on the amount of the incorporated air or added liquid media. Since wet foam is thermodynamically unstable, it decreases the overall energy of the foam by Ostwald ripening and this situation causes to increase in the size of bubbles hence the pores in the final products are very large. Initially, stabilization of foams in the precursor is very critical.

There are several ways can be used for stabilization that are stabilization with surfactants and stabilization with particles. Various long-chained amphiphilic and biomolecules like lipids and proteins can be used as surface-active agents for stabilization of wet aqueous foams.

These molecules are slower the coalescence and chemical reaction of bubbles by adsorbing on the air- bubble surface and reducing air-water interfacial energy. But these agents cannot prevent the stabilization for a long time after foaming. Hence

surfactants which are for direct foaming need setting agent that consolidates the microstructure of foams before coalescence and chemical reaction occur [1].

The fabrication route of macroporous ceramics by direct foaming method is given in Figure 1.5.

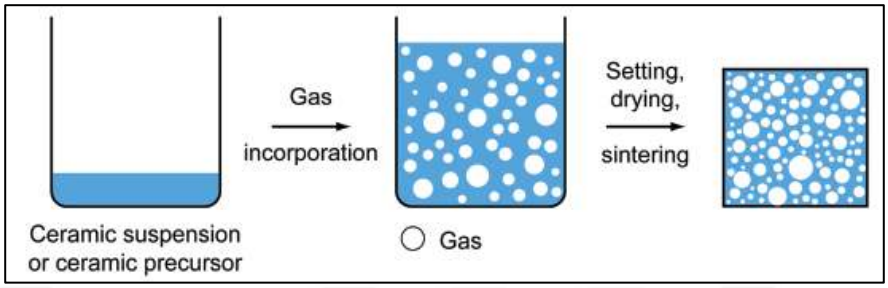

Figure 1.5 Incorporation of gases or foaming agents into the ceramic suspension or precursor [1].

The comparison of the final pore sizes and pore characteristics were given in Table 1.1 for all three methods.

Table 1.1 Relationship between the pore characteristics and production technique [1].

	Replica Method	**Sacrificial Template**	**Direct Foaming**
Pore Size	200 µm- 300 µm (synthetic) 10-300 µm (natural)	1-700 µm	35 µm- 1.2 mm
Porosity (%)	40-95 (synthetic) 25-95 (natural)	20-90	40-97

As seen on the Table 1.1., the range of the possible obtainable pore size is wider than the other techniques which makes the pores more tailorable in the sacrificial template method. The porosity range depends on the replicated materials for replica technique

however for sacrificial template method wide porosity range can be obtained. In direct foaming method, the pore size range is wider than the other two techniques.

1.2 Gradient Porous Ceramics

A ceramic component including pores with different pore characteristics called as graded/gradient/hierarchical porosity. This type of structured ceramics can be specialized based on its applications and these materials have wide range of properties like fluid transportation, rapid thermal cycling possibility, chemical and mechanical stability and efficiently using.

Graded porous ceramics have various industrial applications which include catalysis, gas or liquid filtration, extraction, separation, sorption and scaffolds for biological applications.

On the other hand, graded porous ceramics have some particular limitations that are mechanical strength, difficulties in the controlling of length scales and achieving these complex structures [2].

The schematic representation of gradient porous ceramics is given in Figure 1.6.

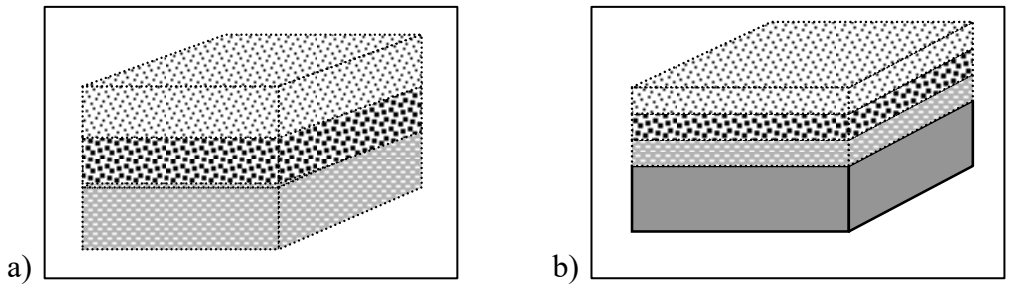

Figure 1.6 Illustration of graded porosity (a) with a porous layer and (b) with a dense layer [2].

Gradient porous materials can be generally produced in two types that are with and without dense layer which was shown in Figure 1.2.

1.2.1. Production of Graded Porous Ceramics

In the fabrication of graded/gradient porous ceramics, various templating objects such as microspheres, colloids and/or emulsions can be used to have pores with different length, shapes and types. Gradient porous ceramics are produced by templating twice with the using of large colloids and small or supramolecular aggregates. Comparison to the synthetic materials, biological templates are also used to fabricate graded/gradient porous ceramic components. The obtained porous structure by using of biological template method cannot be achieved by the synthetic template methods.

The biological templates have its unique porous structures and morphologies. In general, biological templates are inexpensive, renewable, environmentally free of hazard. Starch gel, palm fibers, cuttlebone, diatoms, plants, etc. are the natural complexes and have been used as templates. The incompatibility between the synthetic ceramic precursor and the biological component is the limitation.

One way to produce hierarchical porous ceramics is impregnation of polymer foam. These foams can be found in different composition, pore size and pore morphologies; and they are usable foams to introducing the graded/gradient structure into the ceramic components. They are inexpensive and available. Polyurethane (PU), polystyrene (PS) and urea-formaldehyde (UF) can be said as a porous material used to produce hierarchical porous components.

Using of emulsions is another way to produce graded porous ceramics. Due to the latest researches on the usability of emulsions at now, prompted to decrease ordered structures with limited number of defects.

Besides that, if the hard-colloidal components are used as a templating element, the reachable maximum pore size is bordered to the colloidal dimensions. This issue is a heavy limitation because of diffusion of the solids which is a requirement. The other disadvantage of using hard- colloids is shrinkage during drying, condensation and densification of the ceramic component which can cause to cracks and pulverization. Adopting the strategy of templating due to emulsion system can be a solution for this. As an emulsion, water, oils, etc. can be used.

1.2.2 Tape Casting of Porous Ceramics

The fabrication of the graded/gradient porous ceramics needs to control the pore characteristics such as size, size distribution, morphology and connectivity in 3D and tailoring these properties can be achieved by several synthetic routes.

Well-known ceramic forming methods such as pressing, extrusion, gel, slip and tape casting are applicable for the production of the graded/gradient/hierarchical porous ceramics [2-5]. Tape casting is commonly used technique for shaping of ceramics. This technique is casting of a tape which is in the form of pseudoplastic suspension or named as slurry. This slurry generally includes inorganic powder, liquid for dispersion of powder, organic additives (binders, dispersants, plasticizers) which acts as solvent and medium for dispersion of powder.

Liquid also controls the viscosity of the slurry and works as a vehicle for distribution of the additives and dispersion of powders homogeneously. Dispersants work as deflocculant and prevent the settling of powders. Binders keep the ceramic particles together until sintering process and they should be removed by heat-treatment. Plasticizers have a duty to increase the flexibility of the green tape [35].

Slurry for tape casting should satisfy some criteria to increase the quality of the tapes that are no defects during drying, microstructural homogeneity, good lamination, easy debinding and high mechanical strength after heat-treatment. This satisfaction is provided by the adjusting of the amount and properties of binder, addition order and concentration of solids. Also, these parameters have an effect on the density, porosity, thickness, quality of surface and mechanical properties. Pseudoplasticity is required to obtain homogeneous tapes where viscosity decreases because of the shear forces between blade and the casting area. Just after that, the viscosity increases to take control of the flow and prevent the particle sedimentation [35].

The slurry is poured onto the polymer type and a blade or its well-known name is “Doctor Blade” is responsible with the giving a thickness to the tape. Then, the green tape is left to the drying until the tape become semirigid and flexible.

This multilayer structure is fabricated by applying pressure by sticking the tapes at temperature that is below the boiling points of the binders and plasticizers [6].

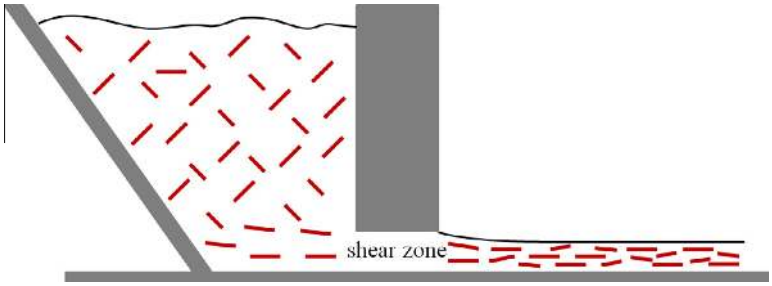

Figure 1.7 Illustration of shear forces for tape casting [10].

As mentioned previously, producing of graded porous ceramic materials can be produced by tape casting method. Producing porous ceramic bodies by tape casting can be done with four different ways that are tape casting with sacrificial template, phase inversion tape casting, freeze tape casting and partial sintering.

Sacrificial pore formers are added into the slurry and they are removed with evaporation and/or burn-out processes and after this process, the remaining place called as pore. In general, these sacrificial pore formers can be some synthetic (fibers, polymer beads) and natural organic materials (starch, cellulose) or liquids (water, emulsions, gel) [2,5].

To produce tailored porosity, it is usually chosen to use only components designed to behave as pore former in the slurry. Using of this kind of materials permits to fabricate a very wide and easy to control range of porosity, related to amount, shape, size and distribution of the pore formers. This range constructs positive linear relationship between amount of the sacrificial pore formers and total porosity. This situation is known because increment of the sacrificial pore content results in leakage network between the particles. In addition to this, mixing of the pore formers with slurry also has significant effect on the formation of pores. Mixing method and milling time changes the pore size distribution into narrow range [2,5].

1.3. Hierarchical Porosity in Nature and in Bioceramic

Hierarchical porosity can be seen in nature very common. The peel of pomelo fruit, marine sponge and bone have hierarchical porosity and they are well-known examples.

Peel of the pomelo fruit has hierarchical porosity. In the detailed imaging shows that there are foam-like structures and inside of the foam-like structures, there are some liquid-filled cells. The hierarchical porous structure of pomelo fruit peel can be seen in Figure 1.8.

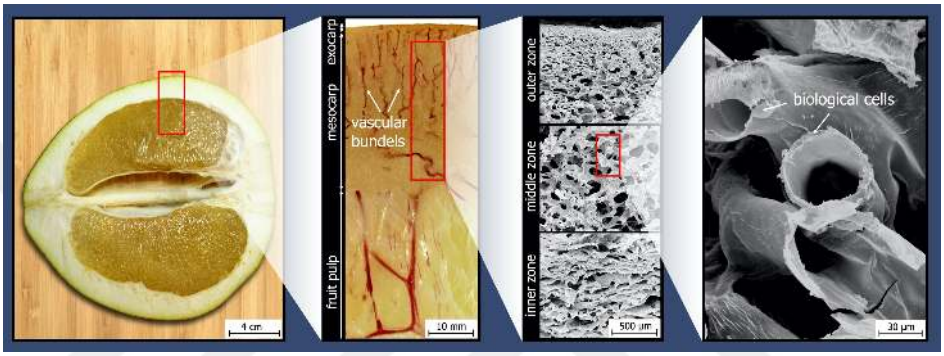

Figure 1.8 Peel of pomelo fruit with hierarchical porosity [47].

Marine sponge has also hierarchical porous structure. Cross-section of the marine sponge walls have canals and these canals have porosity. When these porous canals detailed, there are other porosities in these pores. This hierarchical porous structure of marine sponge is given in Figure 1.9.

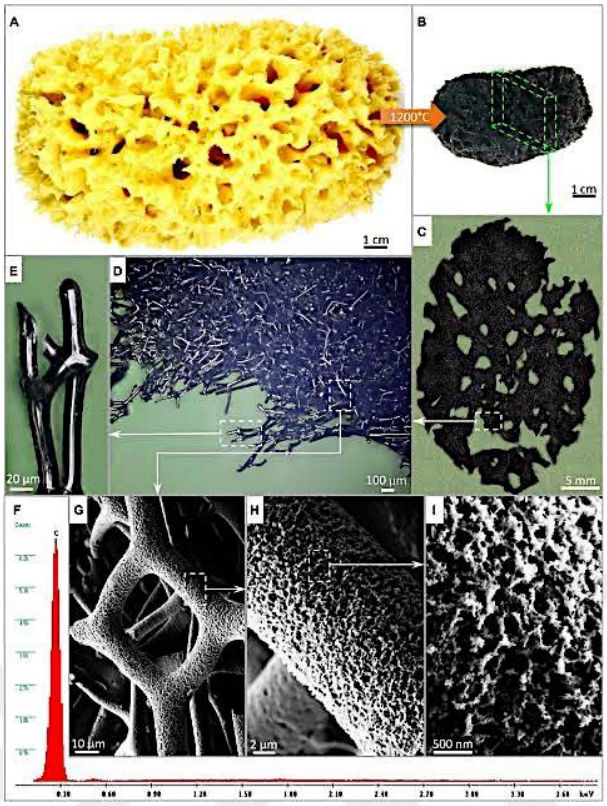

Figure 1.9 Hierarchical porous structure of marine sponge [48].

Bone has multiscale porosity for come through the mechanical loads and reducing the energy lost during locomotion. Bone tissue shows a core-shell structure and the core formed as foam-like material called as trabecular and shell has denser structure with isolated pores and interconnected canals which is known as cortical bone.

The trabecular bone reduces the total weight of the bone and gives spaces for the blood vessels and marrow. Long channels in the cortical bone permits the tissue vascularization. Overall the canal networks and the pores enable the transportation of the cells, nutrients and the ions.

The gradient porous structure illustrated in the Figure 1.10.

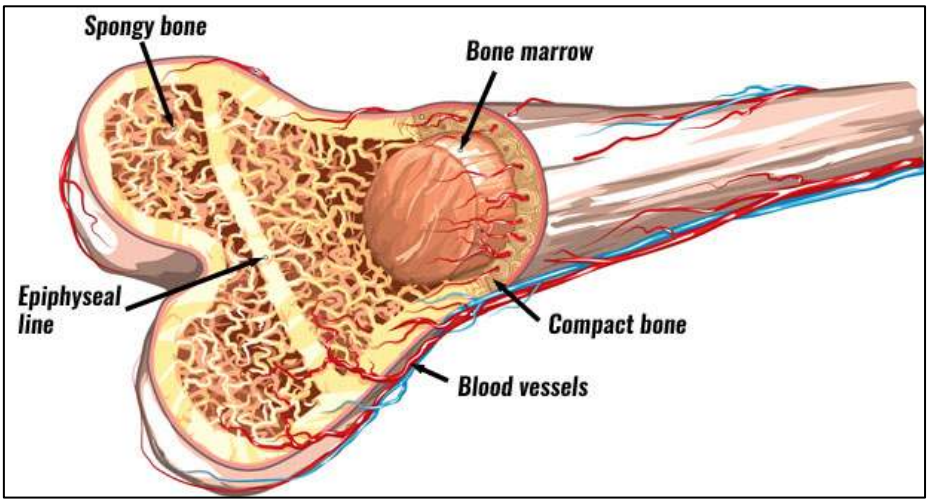

Figure 1.10 Hierarchical porous structure of bone [10].

1.4. Bone Grafting Materials

Bone has a structure with connective tissue which includes cells, fibers and substances. Differently from other connective tissues, bone has mineralized extracellular components which brings strength and rigidity to bone.

All bones in the human skeletal system can be divided macroscopically into two different types that are cortical and trabecular. These tissues have the same matrix compositions, but they are different in terms of structure and function.

Cortical bone has the 80 wt. % of total skeletal tissue mass and cortical bone has high matrix mass per unit volume and low porosity which is between 5-15%. These properties give high compressive strength to the cortical bone. However, this porosity allows nutrients and vascular and neural supplements.

Porosity increases by aging, disusing or overusing or disease situations. Porosity degree is an important factor for fracture because increasing in intracortical porosity can result in decreasing in bone strength.

On the contrary to cortical bone, trabecular bone has high porosity which makes the 50%-90% of total trabecular bone volume. The porosity of the trabecular bone is between 40-95%.

Pores dispersed in an order for both vertical and horizontal directions in a rode-like shape which give spongy-like structure to the trabecular (spongeous) bone.

This structure reduces the compressive strength of the trabecular bone because it has low matrix mass per unit volume. However, this situation is functional because this gives high surface area for red bone marrow, blood vessels and be in contact with bone and connective tissues. Beside the low strength of the trabecular bone but it has a role on the internal support. With this mechanical support load distributes and energy adsorbs [13-15].

On the Table 1.2, the some of the physical properties that are porosity, pore size and mechanical properties were given.

Table 1.2 Properties of human cortical and cancellous bone [16].

Property/Bone	**Cortical Bone**	**Cancellous Bone**
Porosity (%)	5-10	75-80
Pore Size (µm)	10-50	300-600
Compressive Strength (MPa)	110-150	2-6
Young's Modulus (GPa)	18-22	0.1-0.3

As seen on the Table 1.2., the mechanical properties decrease due to the increasing on the pore size and porosity where cancellous bone is the inner and more porous section of the bone while cortical bone is the outer and less porous section.

Ideally, bone substitute should be biocompatible and should not cause any negative inflammatory answerback. Filling the spaces which is occurred by the removing defected bone should not be difficult and should not take long times. The bone substitute should have osteoconductive and osteoinductive behavior. It should be observable in vivo or should be radiolucent to allow radiographic evaluation. Besides, the bone substitute should be thermally nonconductive and sterilizable. The structure of bone functionally different in the meaning of porosity from the surface cortical bone through the inner cancellous bone.

For this reason, during the designing of the implant materials with the gradient porosity should be considered for the mimicking as far as possible the bimodal structure of bone.

Using of substitutes for bone increases particularly for oncological surgery, traumatology, prosthetic surgery, revision and spine surgery.

Bone substitute can be described as an organic or a synthetic material or the combination of them which are inserted to the bone for the curing or healing defect of the bone rather using of autogenous or allogenous bone [6, 10].

Bone substitutes can be classified into three categories that are bone grafts (autograft, allograft, xenograft), ceramics based (hydroxyapatite, TCP, calcium sulphate) and growth factors (DBM, PRP).

1.4.1 Autografts

Autografts have the gold standards for the bone substitution. Autologous bone grafting contains the use of bone from the same tissue obtained the graft. Autogenous bone has both properties that are required for formation of bone; the properties are osteoconductive, osteoinductive and these bone grafts allow growth factors and osteogenic cells with no infection hazard. Autologous bone is replaced carefully to the fractured bone. Requirement of surgical site donor and blood loss, hematomas, infection, fracture, possibility of pain after operation are the disadvantages of the autografts.

1.4.2 Allografts

Allografts are reproduced from humans like autogenous and they also show proper alternative to autogenous bone. Differently from autogenous, allografts should be processed in bone tissue banks. Allografts are osteoconductive but their osteoinductive properties are weak. Allografts needs sterilization by using of gamma irradiation and this type of sterilization has harmful effects to mechanical properties and it causes protein deactivation.

1.4.3 Xenografts and Other Bone Substitutes

Xenografts have different origin like bovine bone, and they can be freeze dried, demineralized and deproteinized. Xenografts are often dissipated calcified matrix.

Corals are harvested and processed to come in “coral derived granules (CDG) and different types of xenografts. Coral based xenografts are primarily calcium carbonate meanwhile calcium carbonate is found in hydroxyapatite.

The coral is transformed to hydroxyapatite under hydrothermal processes. Xenografts have shown good results in dentistry but rare approval in orthopedics.

Demineralized bone matrix (DBM) is produced from processing of banked donor bone. Decalcified bone matrix is typified by the collagen matrix that is assumed to pair the unique tridimensional structure of the bone with housing to host cells for invasion, differentiation and growth of them.

In addition to DBM, bone morphogenetic proteins (BMP), insulin growth factors (IGF), transforming growth factors (TGF) and fibroblast growth factors (FGF) are able to evoke activation of osteogenic stem cells and progenitor cells.

In platelet rich plasma (PRP), platelets are collected from blood plasma and they are a rich source for growth factors. PRP is simply gotten from autologous blood platelet by gradient density centrifugation. However, PRP is not suitable alone for bone substitute [13-15]

1.4.4 Ceramic based Bone Substitutes

In general, ceramic based bone substitution materials are mix of hydroxyapatite (HA), tricalcium phosphate (TCP) and the amorphous phase of HA. HA is relatively inert which sustained in vivo for extended periods of time, though TCP, which is more porous than the HA, propagates biodegradation within 6 weeks in the placed area of bone. HA has very high mechanical strength, but mechanical properties of TCP is weak. Based on concentration, of HA and TCP the strength values are between 10-60 MPa which is lower than the compression strength of cortical bone (150-200 MPa) and this is limitation of the ceramic based biomaterials.

Ceramic based biomaterials for the usability in the bone tissue should have some properties such as bioactivity, biocompatibility, chemical and biological stability, mechanical compliance and porous structure.

Both of these properties have an importance, but porosity have a key role on the bone tissue ingrowth, permitting the cell penetration, easing the vascularization and transportation of the nutrients.
In order to having these situations, the scaffold should have interconnected pores with a large surface-to-volume ratio and pores size of the scaffold should be at least 100 μm in diameter which number is ideal to repairment of bone.

Hydroxyapatite is a frequently used biomaterial and it is also found in the component of the bone. Hydroxyapatite ceramics with gradient porosity have potential application areas such as mimicking the bimodal structure of the cortical and cancellous bone, for gaining the mechanical strength to the bone and permitting cell/tissue ingrowth, scaffolds for tissue engineering and drug delivery systems, spinal fusion cages which need mechanical strength and osteointegration. Another graded porous ceramic based biomaterial is Al_2O_3-ZrO_2 composite materials and they developed for the both mechanical strength and osteoconductivity [13].

1.5 Si_3N_4 Ceramics in Bioceramic Applications

Silicon nitride (Si_3N_4) ceramics have been used and preferred in several industrial and high-technology applications because of the its combination of properties that are chemical, thermal, tribological and mechanical properties. With all that properties, the possibility of usage of Si_3N_4 as a bone substitute or and implant was proven [17].

The density of Si_3N_4 is 3.17 g/cm^3. At the temperature of 1877º C, Si_3N_4 decomposes to liquid silicon and nitrogen gas. The basic structural unit of Si_3N_4 is highly covalently bonded SiN_4 tetrahedra and these tetrahedra structures can be connected in different paths for the formation of three different modifications. Due to this highly covalent bonding, there can be requirement for sintering additives which helps the densification. In general, the densification of Si_3N_4 can be done by pressureless sintering, sintering under gas pressure, hot pressing and hot-isostatic pressing.

The sintering additives are often metal oxides mostly rare earth oxides. The densification process is explained as a liquid phase sintering.

At elevated temperatures, SiO_2 which is always found in the surface of Si_3N_4 reacts with additives for the formation of melt oxides and in the increment on the temperature, an oxynitride in the melt form dissolved by Si_3N_4.

Si_3N_4 has three polymorphs. The two polymorphs are in the form of hexagonal (α-Si_3N_4 and β-Si_3N_4) and the other polymorph is in the form of cubic structure (c-Si_3N_4). The c-Si_3N_4 can be obtained under high-pressure and high-temperature. Most of the Si_3N_4 ceramics are produced by α- Si_3N_4 and this transform to β-Si_3N_4 during sintering (1500-1700°C) process [49]. During this transformation, the shape of grains changes to elongated needle-like grains. The ratio of β phase is depends on the initial α/β ratio which is found in the starting powder.

This transformation gives great opportunities to advanced engineering applications. However, the microstructure of the Si_3N_4 does not directly depend on the initial β content.

Some experiments about the mechanical properties in the meaning of fracture toughness of the Si_3N_4 ceramics was showed that the fracture toughness increases with the volume fraction of elongated grains. However, the high fracture toughness does not only depend on the grain morphology, another requirement is grain boundary phase [16-17-18].

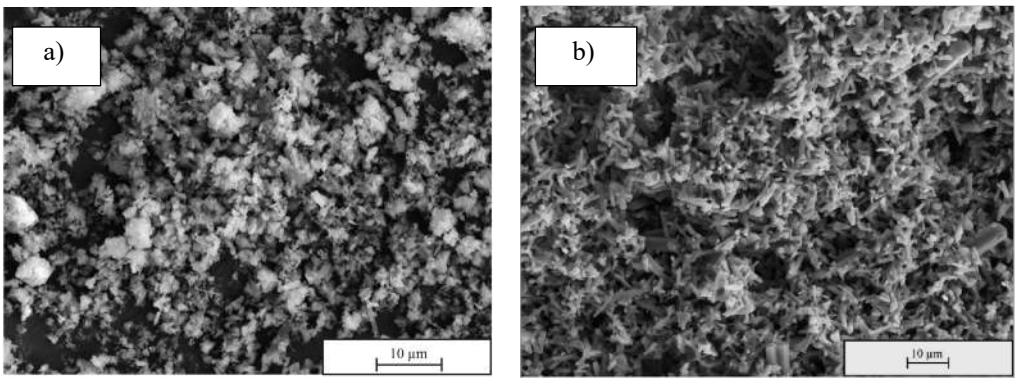

Figure 1.11 SEM of (a) α-Si_3N_4; (b) β-Si_3N_4 [42]

SEM images of the α-Si_3N_4 (a) and β-Si_3N_4 can be seen in Figure 1.11. The evaluation and final characteristics of β-Si_3N_4 depends on the starting powder where the formation of rod-like β-Si_3N_4 grains is strongly correlated to the using of α-Si_3N_4 as a starting powder and due to the rod-like grains, interconnected three-dimensional network structure can be occurred [33].

The crystal structures of trigonal α-Si_3N_4 and hexagonal β-Si_3N_4 structures are illustrated in Figure 1.12.

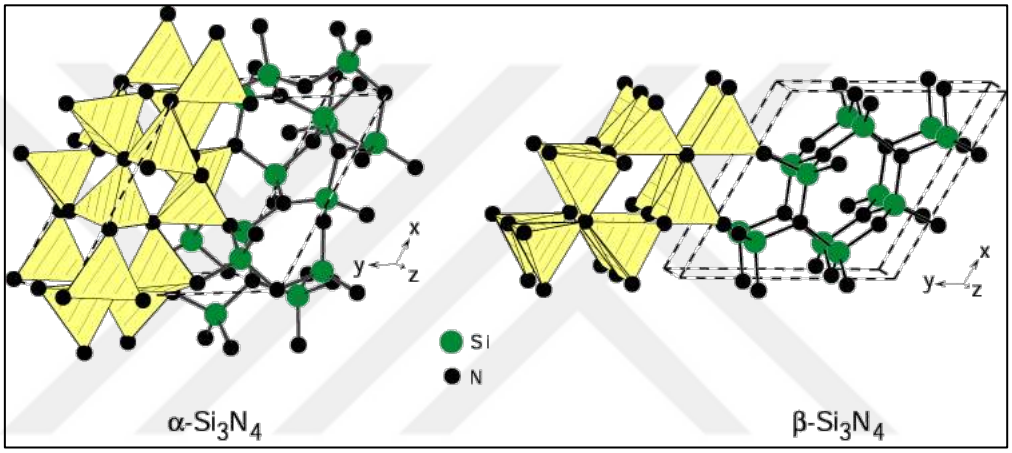

Figure 1.12 Schematic illustration of crystal structure of α and β-Si_3N_4 [20]

The trigonal α-Si_3N_4 phase transformed to the hexagonal β-Si_3N_4 phase at elevated temperatures where during this transformation the Si_3N_4 is denser than the α phase.

Beside the studies that were done on the dense Si_3N_4 ceramics as a biomaterial, also the possible usability of porous Si_3N_4 ceramics in bone replacement applications was proven. In various studies, the porous Si_3N_4 was produced by several methods such as reaction bonded (RBSN), replica technique and pore former addition (sacrificial template method).

Si_3N_4 ceramics are widely used as thoracolumbar interbody spinal fusion devices and cervical interbody fusion devices.

Beside vertebral applications, also Si_3N_4 ceramics have a possibility to using as a hip, knee joint element and in dental applications. This wide usage due to the kind behavior of Si_3N_4 in the biocompatibility experiments. The Si_3N_4 shows achieve fine bone growth with the antibacterial resistance based on in vitro and animal studies. These studies were done through the clinical investigation and osteoconductivitial, osseointegrational osteoinductivitial properties. These investigations and properties proven the biocompatibility of Si_3N_4. The osteoconductivitial, osseointegrational osteoinductivitial properties were analyzed by culturing of living cells on the surface of Si_3N_4 ceramics and culturing of bone tissue through the surface of Si_3N_4 ceramics.

The reasons of biocompatibility of Si_3N_4 are shown in Figure 1.13. The surface properties of the Si_3N_4 is a key factor for cell adhesion antibacterial resistance.

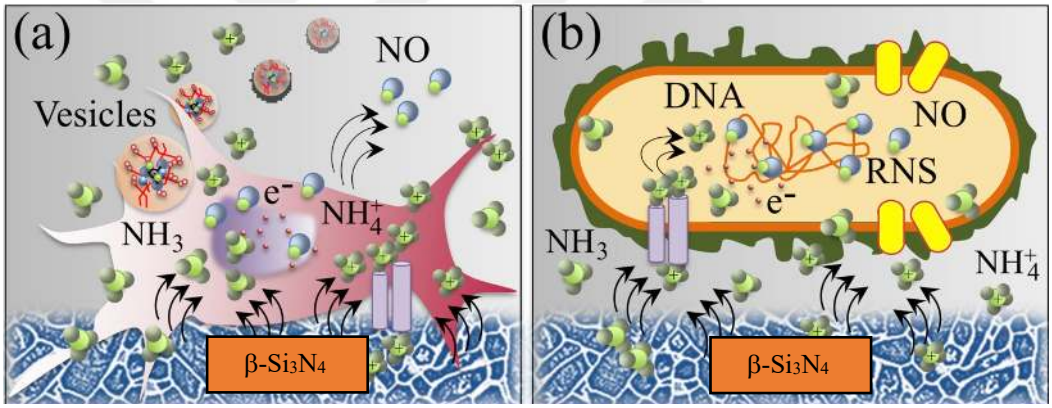

Figure 1.13 a) Cell adhesion and surface properties of β-Si_3N_4 and, b) antibacterial properties of β-Si_3N_4 [48].

The surface of the β-Si_3N_4 has a unique property which effects the osteoblast cells in a positive manner, but the bacteria are affected in a negative way which is very advantageous.

The surface of β-Si_3N_4 releases NH_3 ions and these ions are used by the cells as a nutrient and these ions are disintegrated to the NH_4^+ ions to fabricate NO where NO is a signal for osteoblastogenesis.

This process can be seen on the figure 1.13. a). But NH_3 has a negative effect to the bacterial cells and NH_3 does not allow the attaching and growing of the bacterial cells.

Table 1.3 summarizes the studies about bone replacement and implantation applications for both dense and porous Si_3N_4 ceramics.

Table 1.3 Literature review of biocompatibility studies of Si_3N_4 ceramics

Howlett et. al. [22]	1989	The first study about usability of Si_3N_4 ceramics was researched in 1989. Silicon powder was milled with alumina balls and this powder were mixed with ground silicon. For having interlinking porosity, this silicon powder was mixed with PMMA beads. During gas flow, increased gradually to 1450^oC and sintered at this temperature for 20 hours. By this way, silicon powder with PMMA beads was nitrided and silicon nitride with interlinking porosity was obtained. For the in vivo characterization, marrow stromal cells from the primary source was used and cells were seeded onto the Si_3N_4 surfaces. After cell seeding, the cells started to grow, and cells differentiated into bone, cartilage and fibrous tissue.
Sohrabi et. Al. [23]	1999	The aim of this study was to investigate the effects of Si_3N_4 ceramics on the human osteoblast-like cells (MG-63) in vitro. Sintered reaction-bonded and reaction-bonded Si_3N_4 ceramics were used for this study. The cytotoxicity was analyzed by the expression of IL-1β and TNF-α and compared with the control cells. As a result, cells propagated on the surface of sintered reaction-bonded samples and they had the same IL-1β and TNF-α as in the control cells. Hence, Si_3N_4 did not show any inflammatory effects and showed biocompatibility.

Table 1.3 (Continued) Literature review of biocompatibility studies of Si_3N_4 ceramics

Silva et. al. [24]	2004	Si_3N_4 (91 wt. %) powder with Y_2O_3 (3 wt. %), Yb_2O_3 (3 wt. %) and Al_2O_3 (3 wt. %) were ground in an attritor mill with an isopropanol alcohol. Samples were sintered at 1750°C for 1 hour under nitrogen atmosphere. The cytotoxicity experiments were carried out for two different samples which included 90 wt. % Si_3N_4, 6 wt. % Al_2O_3, 4 wt. %Y_2O_3 and 91 wt. % Si_3N_4, 3 wt. % Y_2O_3, 3 wt. % Yb_2O_3 by using of Chinese hamster ovary K-1 cells within the RPMI-FCS culture medium. After cell culture, samples showed noncytotoxic behavior due to live/death cell ratio.
Neumann et. al. [25]	2004	Five different Si_3N_4 ceramics were chosen for in vitro analysis. The sintering method of the 1st and 5th was disclosed; 2nd was sintered under gas pressure; 3rd was sintered reaction bonded; 4th was sintered under atmospheric gas pressure. L929 cell line (aneuploid fibroblast which was isolated from subcutaneous tissue of mice) was chosen. Results had shown that surface properties have strong effect on the cell proliferation. Cells proliferation was higher on the polished surfaces. Reaction bonded sintered samples had very low number of cells.
Silva et. al. [26]	2007	Si_3N_4 (91 wt. %) powder with Y_2O_3 (3 wt. %), Yb_2O_3 (3 wt. %) and Al_2O_3 (3 wt. %) were ground in an attritor mill with an isopropanol alcohol. Samples were sintered at 1750°C for 1 hour under nitrogen atmosphere. After XRD analysis β-Si_3N_4 grains were found where grains dispersed in a glassy phase. These samples were implanted into rabbit's tibia and kept for 8 weeks. After 8 weeks, implants with surrounding bone tissue was removed and prepared for SEM. SEM

Table 1.3 (Continued) Literature review of biocompatibility studies of Si_3N_4 ceramics

		results showed that newly bone formed around the Si_3N_4 sample and this tissue extended towards the bone marrow.
Mazzocchi et. al. [27]	2008	Dense Si_3N_4 ceramics were prepared with different additions. In the first group, there were 90 vol. % Si_3N_4+ 10 vol. % bioactive glass; in the second group, 91.3 vol. % Si_3N_4+ 8.7 vol. % MgO; and in the third group, 65 vol. % (93 wt. Si_3N_4 + 2 wt. % Al_2O_3 + 5 wt. % Y_2O_3) + 35 vol. % TiN. Both samples were characterized by in vitro cytotoxicity and for this experiment NCTC L929 cell line was used. Both samples, including Si_3N_4-TiN sample, are non-cytotoxic and also TiN is the second reinforcing compound for the formation of the hydroxyapatite.
Bal et. Al. [28]	2012	Si_3N_4 samples were fabricated with Al_2O_3 and Y_2O_3 as a sintering additive and sintered at N_2 atmosphere above 1700°C. For a comparison, some of the samples were produced by using hot isostatic pressure and these samples were polished. Pressure was applied approximately 50 MPa and sintering at above 1700°C. Both samples were characterized with in vitro studies. In this studies, L929-mice fibroblast were used just for polished samples. Human osteoblast-like cell line was used for N_2-sintered samples. Due to MG-63 cells, Si_3N_4 samples showed excellent non-cytotoxicity and L929 used samples showed favorable cell growth, viability and morphology.
Youssef et. al. [29]	2016	The Si_3N_4 ceramics were implanted to the human posterior lumbar spinal fusion and after implantation the CT and dynamic X-Ray compatibilities were investigated. The samples were fabricated by Amedica Co. CT scans and dynamic X-ray evaluations showed that the bone was appeared which was implanted, meaning of this, the Si_3N_4 ceramics have better imaging properties.

Table 1.3 (Continued) Literature review of biocompatibility studies of Si_3N_4 ceramics

Pezzotti et. Al. [30]	2017	Si_3N_4 (with Al_2O_3 addition as sintering additive) samples were characterized by using of SAOS-2 cells and the Si and N elements that are found on the surface of Si_3N_4 samples which increases the metabolic activity of the osteoblast cells that results in efficient bone growth. Surface of Si_3N_4 evokes the cells for producing of bony apatite. This study showed that Si_3N_4 supports enhanced osteogenesis.
Ishikawa et. Al. [31]	2017	In this study, two type of Si_3N_4 were used. Both samples were fabricated by mixing of Si_3N_4, Y_2O_3 and Al_2O_3, then they spray-dried. One group of the samples were different in the meaning of their final heat-treatment and surface morphology. One group was heat treated 1650^oC and above 200 MPa pressure; the other group was heat treated 1700^oC without pressure but both heat treatment processes were done under N_2 gas environment. Grinded samples were held in heat treatment at 1400^oC with N_2 annealing for 30 minutes. Samples were characterized in the meaning of antibacterial properties by using of MRSA bacteria. For the in vivo experiments, samples were kept in USA300 LAC cell culture by overnight and then samples were implanted into the female mice. As a result, Si_3N_4 ceramics showed antimicrobial effects.
Yasemin Tabak Ph.D. Thesis [44]	2018	In this thesis, gradient porous Si_3N_4 ceramics were produced by using of tape casting and pore formers were used in various amounts. The sintering was done at different temperatures under air atmosphere. The cytotoxicity was analyzed by using of human fibroblast cells and the proliferation and number of dead cells were investigated by MTT and LDH tests, respectively. The results had shown that the lower LDH and higher MTT values were obtained for the sample which was sintered at 1400°C.

1.6. Aim of the Study

In this thesis, Si_3N_4 ceramics with gradient pore structure were produced to investigate the potential use as bone grafting material. Density, pore measurement of the samples was done to characterize pore characteristics of the samples. XRD and SEM studies revealed phases existed in the sample and surface/pore morphology. WST-1 and LDH measurements were performed by using osteoblast-like cells to investigate cytotoxicity and biocompatibility of gradient porous Si_3N_4.

CHAPTER 2

EXPERIMENTAL PROCEDURE

2.1 Production of Gradient Porous Si_3N_4 Ceramics

During the production of gradient porous Si_3N_4 based samples, firstly, powder mixture was prepared. 97.5 wt. % Si_3N_4 (UBE SN E10, Japan) was mixed with 2.5 wt. % $CaCO_3$ (Riedel -de Haen, Germany) as a sintering additive which helps densification, Si_3N_4 balls and ethyl alcohol. Both ingredients were ball milled for 24 hours at 180 rpm. Also, the ball milling process provides homogeneous particle size distribution which is beneficial for particle packing and final density and eliminates the agglomerates of the particles. After completion of the ball milling process, the powder was taken out and put to the rotary evaporator.

The general properties of Si_3N_4 ceramics were given on the Table 2.1.

Table 2.1 General properties of Si_3N_4 Powder [18].

Property (UBE SN-E10) Si_3N_4 Powder	**Value**
α-content	> 95 wt. %
SSA (m^2/g)	9≈13

Starting Si_3N_4 powder contains approximately 95% α form and the specific surface area of the powder is approximately between 9 and 13 m^2/g which was given on Table 2.1. The initial state of the powders is important for the properties of the final component and here, the α content has a direct effect on the final microstructure properties.

Partice size distribution of pore formers were characterized by laser diffraction technique (Mastersizer 2000, Malvern Instruments) and results given in the Figure 2.1 for micro-PMMA and Figure 2.2 for PVC. So, the micro-PMMA and PVC was used

as pore formers due to their particle sizes where micro-PMMA has d_{50}= 45 µm and PVC has d_{50}=130 µm. The pore formers also were examined by optical microscope and these are shown in Figures 2.3 and 2.4, respectively.

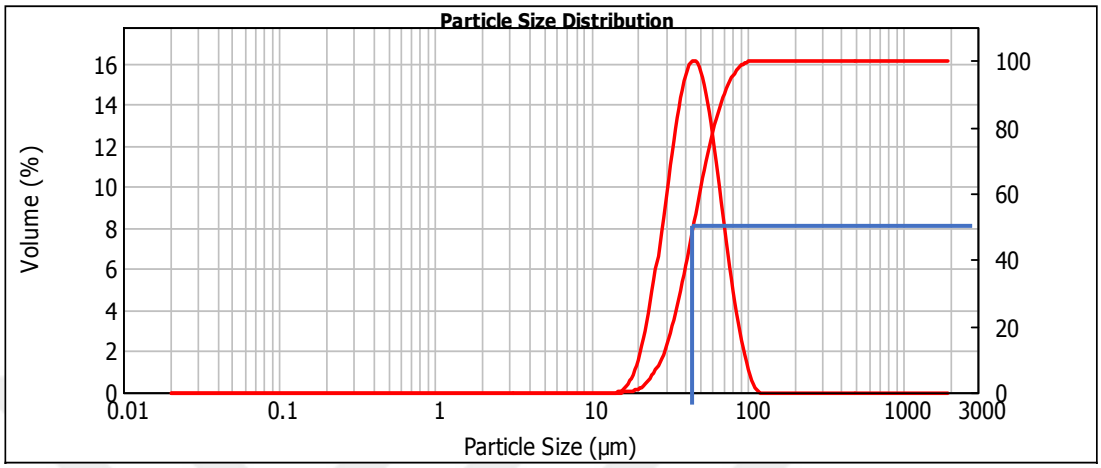

Figure 2.1 Particle size distribution of micro-PMMA (d_{50}=45 µm).

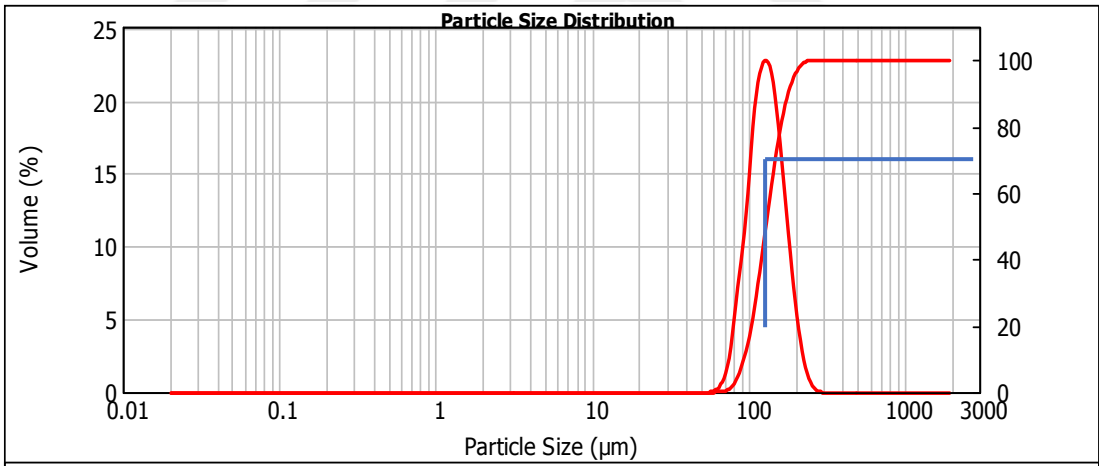

Figure 2.2 Particle size distribution of PVC (d_{50}=130µm).

The Figure 2.3 and 2.4 are the optical microscopy images of the micro-PMMA and PVC. The particle size of the PVC is higher than the micro-PMMA however micro-PMMA has more regular shape. The shape and size differences of the micro-PMMA and PVC can be seen on optical microscopy images, Figure 2.3 and 2.4, respectively. The micro-PMMA has more uniform and circular shape, however the PVC has nonuniform and almost non-circular as seen in Figures 2.3 and 2.4, respectively.

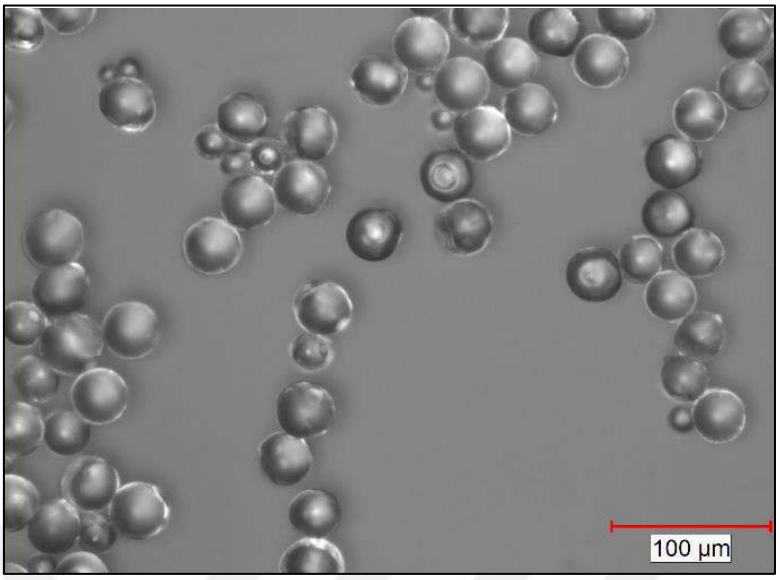

Figure 2.3 Optical microscopy image of micro-PMMA

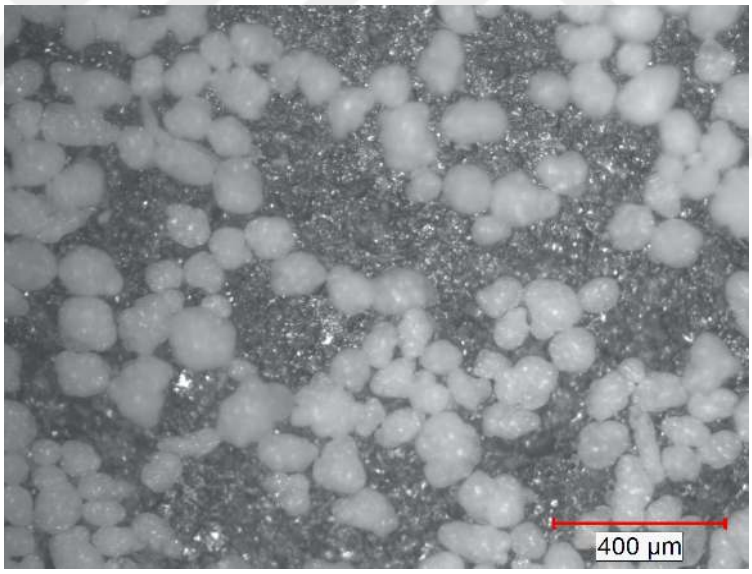

Figure 2.4 Optical microscopy image of PVC

Mostly, for the dispersing the particles, organic and inorganic mediums were used. Water can be chosen as a dispersant but Si_3N_4 develops oxidized surface due to reaction with water, so non-aqueous medium such as alcohol has been used [45].

Firstly, the slurry for the tape casting was prepared. Three different slurries were used which contain Si_3N_4 powder with 5 vol.% micro PMMA and with 5 vol. % PVC and alcohol-based solution with a ratio of (40/60 wt. %) was added to the powder mix. The third solution did not contain any pore forming agent. This solution was mixed by using of speed- mixer (FlackTek, DAC 150.1 FVZ) at 3030 rpm for 7 minutes.

After dispersing of the particles in the solution, the slurry was poured onto the silicone -based Mylar sheet. The tape caster (MSE Technology, Turkey) adjusts the velocity of the DoctorBlade (200 μm) which gives a thickness to the poured slurry and then the slurry became a tape. Then, the tapes were cut into 3 cm x 3 cm piled tape with PVC, tape with micro- PMMA and tape without pore former, respectively. The casted green Si_3N_4 tape can be seen in the Figure 2.5

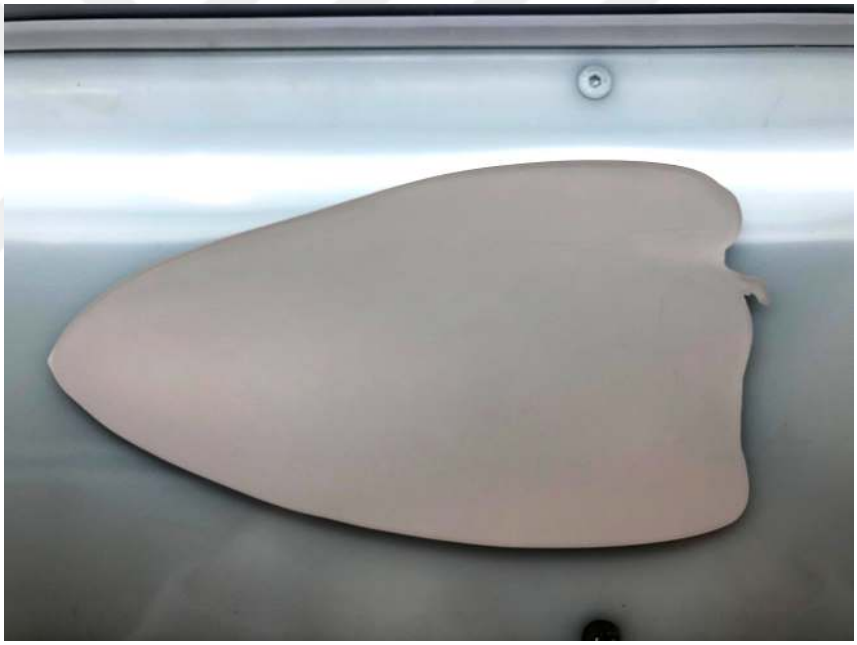

Figure 2.5 Green Si_3N_4 tape.

The surface was smooth and after several trials, the crack free surface and casting were obtained which can be seen in Figure 2.5.

The stacked tapes were pressed under 35 MPa for 15 minutes by uniaxial dry press (MSE Technology, Turkey).

After lamination, samples were heat-treated for removing of the polymeric substances and sintered for the densification. The heat-treatment was done by the gradually and slowly increased temperature which was decided by the TG-DTA analysis of the used pore formers. These analyses were showed in figure 2.6. and 2.7. micro-PMMA and PVC, respectively.

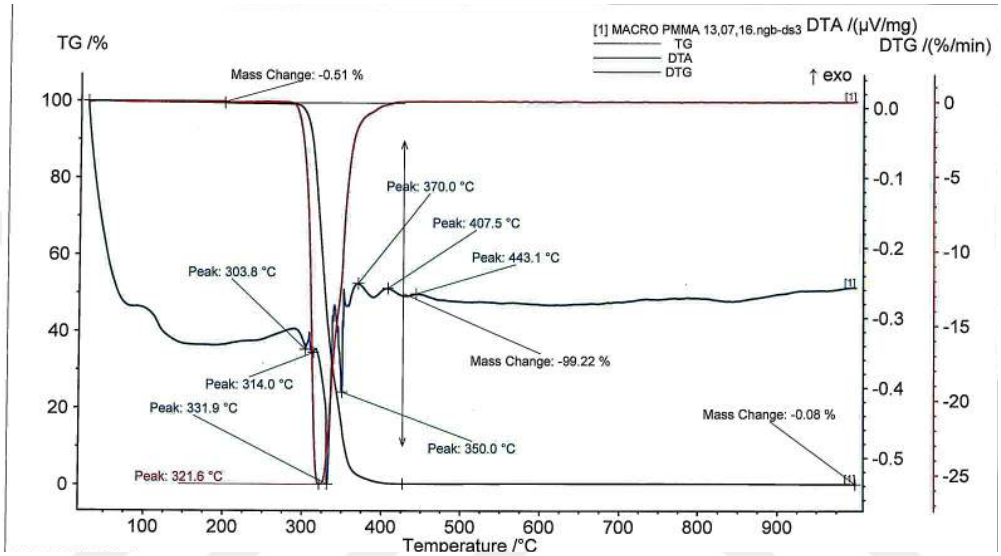

Figure 2.6 TG-DTA Analysis of PMMA

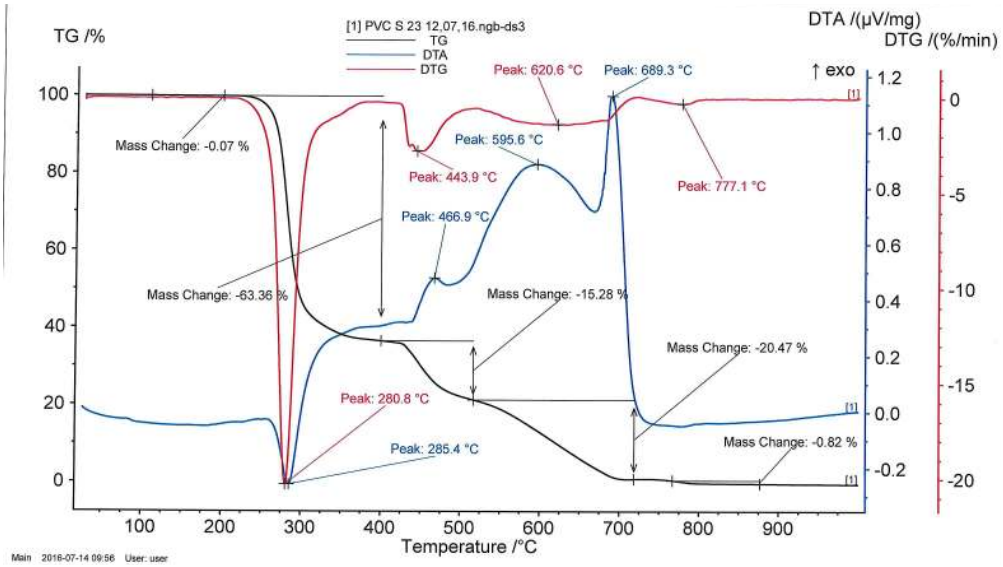

Figure 2.7 TG-DTA Analysis of PVC

The heat rate is very important for the burn-out (MSE Technology, Turkey) process. The TG-DTA analysis were shown in the Figures 2.6 and 2.7, and due to these analyses, the heat rate which will be applied for the burning-out of the polymer-based pore formers was decided This heat rate and maximum temperature decision was done by looking to at which temperature the mass change occurred. The maximum mass change for micro-PMMA was at 440°C which can be seen in Figure 2.6 and the mass change for PVC was completed at 700°C which can be seen in Figure 2.7 The temperature was increased 0.5°C/min up to 750°C and temperature were kept for 1 hour at 750°C. Then, temperature was decreased 5°C in a minute until room temperature. By this gradually temperature increment, the all pore formers and polymeric substances were removed from the sample. Slow heat rate is important for preventing cracks within the sample during burn-out process. In burn-out procedure, the all polymeric substances in the samples were burned-out. By this way, the porous ceramics can be produced which was discussed previously on the sacrificial template method.

After the completion of the burn-out treatment, the samples were sintered. Sintering was carried out under nitrogen atmosphere where during sintering, nitrogen gas flowed. This nitrogen gas flow preventing the formation of SiO_2 formation on the Si_3N_4 ceramics. Gradually heat increment (5°C/mins.) was applied where heat increased up to 1700°C (MSE Technology, Turkey). This gradually heat increment prevent the cracking on the sample and also prevents the furnace linings. At 1700°C, samples were kept for 3 hours, and densification were occurred. The cooling was carried out with same regime.

2.2. Physical and Microstructural Characterization of Graded Porous Si_3N_4 Ceramics

After sintering process, the bulk densities, apparent porosities and impervious volume were determined by Archimedes' principle. The first step is the measuring the dry weights (*D*) of the samples. The second step is boiling of the samples in the DI water. During boiling, the water immersed to the open pores of the samples and the reason of the using DI water is to consider the density of the water as 1 g/cm^3.

The samples were boiled for four hours because the samples were produced with gradient porosity and number of open pores is high. After impregnation of the water to the samples, the samples were held in the same DI water until system cooled down. After impregnation of the water to the samples, the samples were weighed during they were suspended in the water (*S*). After weighing the suspended weight of samples, the excessive water on the surface was removed very kindly by using of smooth linen or cotton cloth to determine the saturated weight (*W*).

The formulas were given in the follows;

$$\text{Exterior volume: } V_e = W\text{-}S \quad \textbf{(2.1)}$$

$$\text{Bulk Density: } BD = \frac{D}{W\text{-}S} \quad \textbf{(2.2)}$$

$$\text{Apparent Porosity: } AP = \left[\frac{W\text{-}D}{W\text{-}S}\right] * 100 \quad \textbf{(2.3)}$$

The pore sizes and pore size distribution of the samples were determined by mercury porosimetry intrusion. The system is based on the non-wetting property and high surface tension of the mercury. The mercury penetrates to the pores by capillary action by applying force and mercury was filled through the pores. The magnitude of applied pressure is proportional to length of the contact line, mercury's surface tension (γ) and the cosine of the contact angle (θ) where any pressure, the mercury intruded pores have a diameter that is greater than [36],

$$D = -\frac{4\gamma\cos\theta}{P} \quad \textbf{(2.4)}$$

The phase analysis of the samples was characterized by using x-ray diffraction (Rigaku MiniFlex). The phase analysis obtained with XRD results was compared with images obtained from scanning electron microscope (SEM) (Hitachi SU5000) analysis. The secondary electron mode was used for visualization.

The elemental analysis was done by the EDX (Oxford X-MaxN 80)

2.3. In vivo Studies

The biocompatibility and cytotoxic characteristics of the Si_3N_4 with graded porosity was evaluated by using of osteoblast-like cells. Before cell seeding, all samples were resized as ~4x4mm in dimensions. Before cell culture, samples were sterilized in autoclave to remove all the contaminants. Osteoblast-like human MG-63 osteosarcoma cell line was used for this study. These cells have similar properties to osteoblast, but they are different from osteoblast cells in some issues that are proliferation kinetic and osteoid production.

Primary culturing of the osteoblast cells requires ethical declarations because the primary cells obtained from the human bone tissue and this process is difficult. Hereby, for this study, MG-63 (ATCC® CRL1427™) human osteosarcoma cell line were used which was already available in the laboratory. This kind of osteoblast-like cells have been used for the biocompatibility and cell culture investigations.

Before *in vivo* studies, cells were defrozen and washed with PBS twice and they were seeded into the flasks for proliferation. Cell culture medium was high glucose Dulbecco's Modified Eagles Medium (DMEM) with 1% of L-glutamine, 1% of Penicillin+ Streptomycin, 1% gentamicin and 10% of Fetal Bovine Serum. The incubation environment should be 5% CO_2 with 95% humidity at 37.5°C. During proliferation cells reached to confluence and adhere to the surface of the flask (T-75). Cells were thawed with 1 mL trypsin EDTA solution and for the inhibition of trypsin EDTA, 6mL full DMEM was used.

The number of cells for seeding was adjusted as 10.000 cells in 75 µL mix for each sample. The number of cells for seeding was determined by counting cells using trypan blue. The cells were counted using a Thoma slide. Cell stained with trypan blue were accepted as death whereas cells which did not take the dye in accepted as living.

The cell-counting culture media (50 µL) and trypan blue dye were mixed in 1:1 ratio for cell counting. By this way, the number of cells to seed can be determined.

The Thoma slide was shown on the figure 2.8. The thoma slide were visualized by optical microscope and cells can be counted due to the given rule which is illustrated on the figure 2.8.

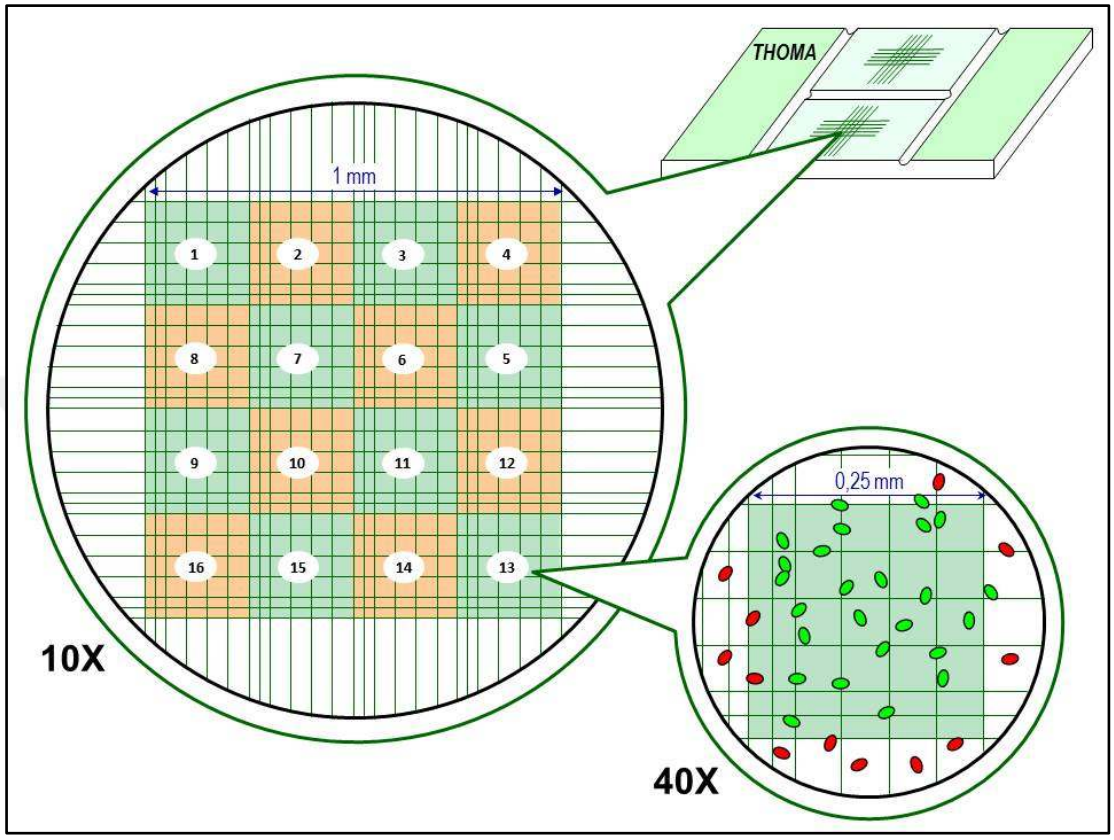

Figure 2.8 Illustration of Thoma slide [38]. The cells which colored green are countable and red colored cells cannot countable.

Cells were counted as 55 in both regions. After counting, the number of cells were calculated as;

$55 \times 2 \times 10^4 = 1.100.000$ cells in 1 mL, **(2.5)**

where 2 is the dilution factor and 10^4 is to determine the number of cells in 1 mL

For each scaffold, 10.000 cells/9 μL DMEM was used.

After cell counting and seeding, the scaffolds were put on the 48- well plate. The placing of the samples into the 48-well plate was schematically illustrated in Figure 2.9.

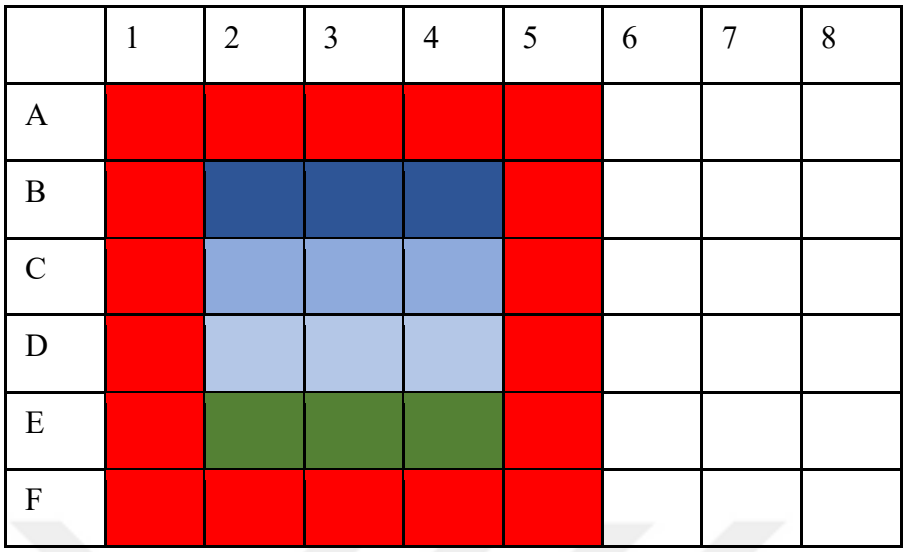

Figure 2.9 Schematic illustration of 48 well-plate and sample placing.

Red labelled wells were filled with full DMEM only to prevent the evaporation of DMEM in the inner wells. Wells labelled in shades of blue and green. Samples were placed as porous side upward direction in all the wells. Samples in the dark blue colored wells were for the 3rd day LDH measurements (3 sample, 1 sample for each well); light blue colored wells were for 7th day LDH measurements; and lighter blue colored wells for 10th day LDH measurements. The green colored wells were for WST-1 measurements and for each green colored well only one sample was used.

After placing of the samples, cells were seeded (75 µL cell mix + full DMEM) and for complete adhesion of the cells, cell seeded samples were incubated for 24 hours. After 24 hours, 215 µL DMEM was added (at final 290 µL) to each well. The cell culture media should not be exceeded 300 µL which is maximum amount of DMEM for 48 well-plate.

2.3.1 Cell Viability

Cell viability assays are commonly used to evaluate cell proliferation and cytotoxicity. In all that both cell viability assays, the important factor is to determine how many living cells there are at the end of the experiment.

There are several methods for describing the number of viable cells such as measuring reduction of tetrazolium, reduction of resazurin, protease markers and detection of ATP.

The reduction of tetrazolium, resazurin and protease activity-based assays measure the general metabolism or enzymatic activity of the cells. Both assays need reagent incubation with a population of viable cells during when a substrate converted into a fluorescent or a colored product which can be detected with a spectrophotometer. Generated color quantity is directly proportional to the number of viable cells. If cells die, the reagent cannot be converted to product [37].

The biocompatibility of the Si_3N_4 samples following in vitro cell culture experiments were evaluated by using WST-1 and LDH.

2.3.1.1 Tetrazolium Reduction Assays

Several tetrazolium salt- based assays were available such as MTT, MTS, XTT and WST-1. However, these compounds are divided into two categories; 1) MTT which is positively charged and easily to diffuse into the eukaryotic cells and 2) MTS, XTT and WST-1 which are negatively charged do not easily diffuse into the cells. The second type of assays used with an intermediate electron acceptor that is for transferring the electrons from the cell cytoplasm to catalyze the tetrazolium reduction into colored formazan product.

2.3.1.2 WST-1 Tetrazolium Assay

Apart from the MTS, XTT and WST-1 are not soluble in the cell cytoplasm, these compounds are directly soluble in cell culture medium. For this kind of compounds, there is no necessity to solubilizing of the formazan and this make MTS, XTT and WST-1 more convenient.

Negatively charged formazan products which helps to solubilization in cell culture medium and this situation limits the cell permeability of the tetrazolium salt.

These tetrazolium compounds were used as intermediate electron acceptor (like PES, PMS) that can saturate live cells and reduced in the cytoplasm or in the cell wall and leave the cell where they convert the tetrazolium salt to the soluble formazan product [37].

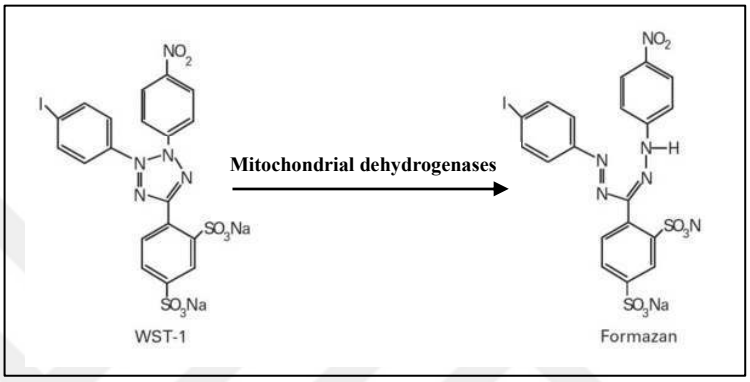

Figure 2.10 Tetrazolium salt WST-1 transform to formazan by cellular mitochondrial dehydrogenases activity.

Increasing on the number of viable cells results in increment on the activity of mitochondrial dehydrogenase then, which causes to increase in the formazan product. The produced formazan product by the viable cells can be analyzed by the absorbance value at 440 nm [37].

For the WST-1 analysis, 29 µL (10% of DMEM in the wells) WST-1 solution was added for each green colored well and incubated for 2 hours.

After 2 hours, 100 µL was taken from each green colored well to the 96 flat bottom well-plate. This process was done under dark environment for preventing the dodging. This well-plate was read (Thermofisher Varioskan Lux multimode microplate reader) at 440 nm. This process was also applied for both 7^{th} and 10^{th} day measurements.

2.3.2 LDH Analysis

Lactate dehydrogenase (LDH) is a common technique for the evaluation of cytotoxic on cells. Briefly, the damage on the cell wall causes release some cytoplasmic enzymes into the culture medium. LDH is a one of the cytoplasmic enzymes and found in every cell. The rapid increment of the LDH in the cell culture medium is clue for the cell apoptosis, necrosis or other types of cell damages.

LDH activity can be easily detected by using of NADH which is produced during the conversion of lactate enzyme to pyruvate for reducing a second compound in a coupled reaction to a product with some properties to quantified easily. This method measures the yellow tetrazolium salt reduction into a red water-soluble formazan-type product by NADH which has absorbance value at 492 nm.

The amount of formazan is related to amount of LDH in the cell culture medium or on in other terms, related to the number of damaged cells [41]. The reversible reaction catalyzed by LDH can be seen in Figure 2.11.

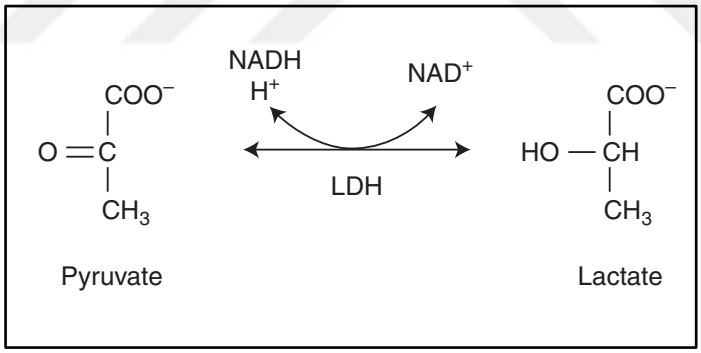

Figure 2.11 Reversible reaction catalyzed by LDH [41].

In 3rd day LDH measurements, the media in the 2B, 3B and 4B wells were collected into Eppendorf tubes and three scaffolds in these wells were taken to the 12 well-plate and prepared for the florescence microscopy. This process was repeated at days 7 and 10. 100 μL media was taken from each Eppendorf to the 96 well-plate and 100 μL LDH solution was added to the media. 100 μL full DMEM was added to the another well.

After that, samples were incubated for 30 minutes and then measurement was done using a multimode microplate reader (Thermofisher Varioskan Lux) at 492 nm. After completion of first measurement, plate was again left to incubation for 30 minutes more. The final measurement at this time was done at 492 nm.

2.3.3 Cell Adhesion and DAPI Staining

Cell adhesion is an important factor for the communication of the cells. The meaning of the cell adhesion is the sticking of a single cell to another cell or onto an extracellular matrix. Cell adhesion needs different requirements for several types of applications and also there is another dependency to specific applications of cells. Biochemical treatment effects and stimulation of the cell culture environment can be said as the methods for the determination of cell adhesion [39].

One of the imaging methods for cell adhesion is fluorescent microscopy. For this imaging, molecules in the cells like DNA or cytoblast can be labelled with a coloring detectable molecule. Generally red fluorescent protein (DsRed2), blue fluorescent protein) (DAPI) and green fluorescent protein (GFP) labelling molecules are used for the fluorescent microscopy.

In this study, DAPI staining performed. DAPI (4',6-diamidino-2-phenylindole) is easily used for fluorescent staining and screening the nuclear DNA for both living and fixed cells. Cells were stained with DAPI according to the manufacturer's protocols. Cell adhesion on the surface of the samples were visualized by DAPI staining.

First, samples (same samples which were in the media used for LDH measurement) were washed with PBS once, but PBS was not added to surface of the samples directly, added and taken from wall of the wells not to damage the adhered cells on the scaffolds. Then, cells were fixed to the surface of the samples by 4% formaldehyde for 30 minutes. Then formaldehyde was removed, and samples were washed again PBS twice. After washing, PBS was added to each well until samples were covered to prevent drying until samples were covered with glass.

The shape of the nucleus of the cell and due to this shape, the behavior of the cell on the surface of the sample can be seen in Figure 2.12.

Cell behavior/ Cell spreading	Viability	Migration	Proliferation	Differentiation
Small 	↓	↓	↓	↓
Medium 	↑	↑	↑	↓
High 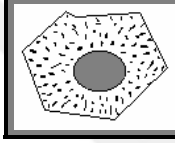	↑	↓	↓	↑

Figure 2.12 Comparison of the cell shape and behavior [46].

The relationship between cell behavior and cell spreading can be seen in Figure 2.12. If the nucleus of the cells is small, cell migration, viability, proliferation and differentiation is lower. When the size and shape of nucleus change to medium size viability, migration and proliferation increases with no change on differentiation. However, size of nucleus and shape of the cytoplasm become high/larger this is a good sign for differentiation.

CHAPTER 3

RESULTS AND DISCUSSION

3.1. Physical Properties of Graded Porous Si_3N_4 Ceramics

The samples were characterized physically in the meaning of density, pore size and pore size distribution. The bulk and relative density and percentage of open porosity values were calculated. The Table 3.1 shows the physical properties of the graded porous samples.

Table 3.1 Physical properties of the samples

	Graded Porous Samples
Bulk Density (g/cm^3)	1.63 (±0.12)
Open Porosity (%)	58 (±2.62)
Relative Density (%)	52

As seen on the Table 3.1., densities of the samples were very low from the theoretical density of Si_3N_4. The reason for this finding the porous structure of the samples. On samples both connected and non-connected pores can be found, and which effected the percentage of the open porosity. The relative densities were calculated by the diving of the bulk densities by theoretical density of Si_3N_4 ceramics which is 3.17 g/cm^3. The density and open porosity values had supported each other.

The pore size distribution of the samples was analyzed with mercury porosimeter (Micromeritics). For the graded porous samples, the pore size distributions were analyzed. Pore size distributions of graded sample can be seen in Figure 3.1.

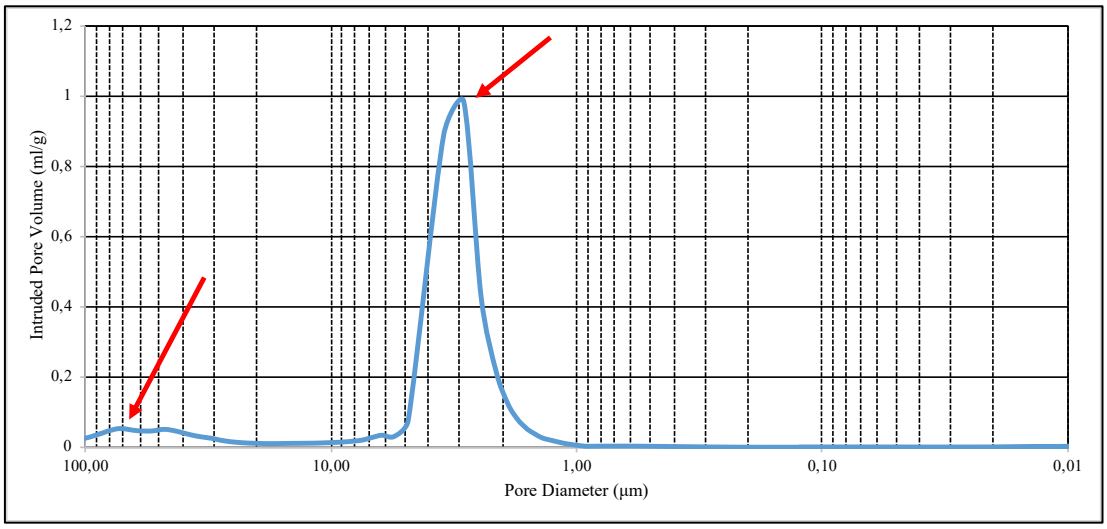

Figure 3.1. Pore size distributions of the graded porous samples

The curve has two peaks can be seen in the Figure 3.1 which is called as bimodal porosity for porous bodies. This bimodal porosity was expected because of the graded porous structure of the samples where two different pore sizes were found in the sample. Red arrows in the Figure 3.1 shows the peaks on the curve.

3.2. Microstructural and Phase Analysis of Graded Porous Si_3N_4 Ceramics

The microstructural analysis of the samples was investigated by X-ray diffraction and the test was done between 10º and 60º 2θ degrees because the major phase which is β-Si_3N_4 can be seen in that range. The XRD graph of a gradient porous Si_3N_4 samples was given in the Figure 3.2.

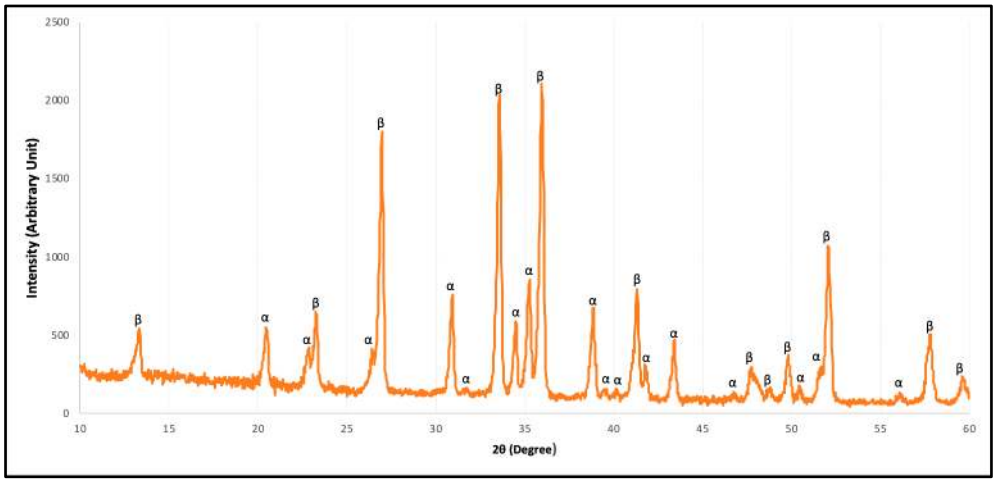

Figure 3.2 Phase analysis of the samples

β phase was seen intensive but α phase could be seen in the Figure 3.2. This showed that sintering temperature or time was not enough for the transformation α to β phase.

Samples were visualized by SEM from the cross-section of the samples and surface of the samples. The cross-section of the non-graded porous Si_3N_4 samples can be seen in Figure 3.3.

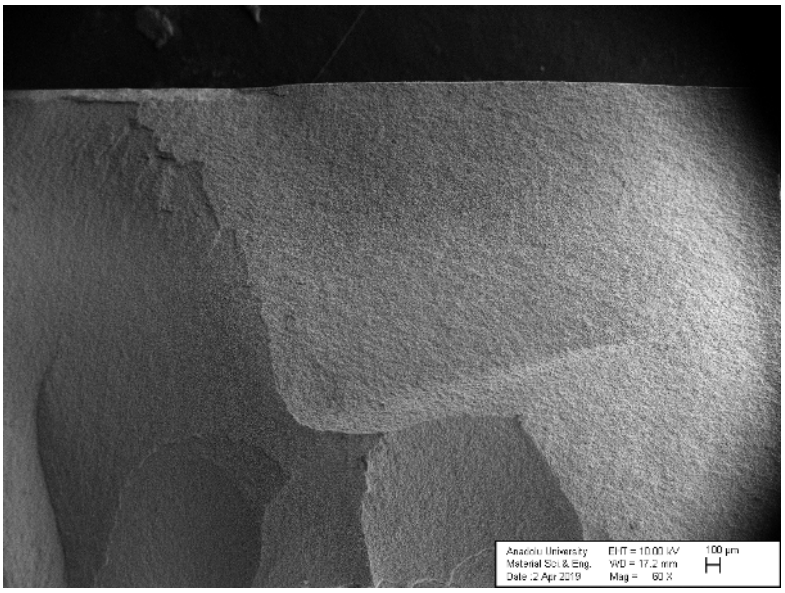

Figure 3.3 Cross-section of non-graded porous Si_3N_4 samples.

The cross-section of non-graded porous Si_3N_4 samples can be seen in the Figure 3.3. There were no pores on the cross-section of the sample. Different planes occurred and cracks can be seen.

The cross-section of the graded-porous Si_3N_4 samples can be seen in Figure 3.4.

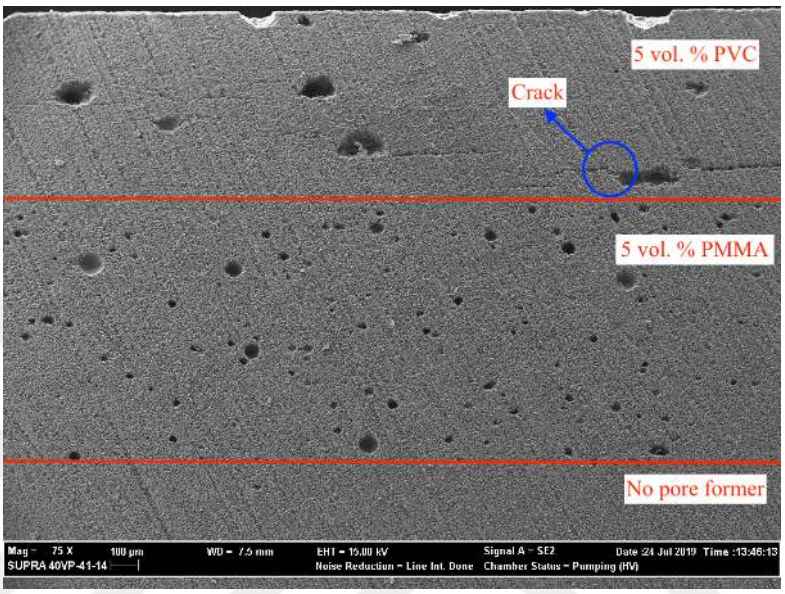

Figure 3.4. Si_3N_4 samples with gradient pore structure.

Gradient/hierarchical porous structure was obtained, and pore sizes and pore structures changed from bottom to the top which was observed in the Figure 3.4. Also, the crack occurred where the upper section (5 vol. % of PVC) which was circled in the Figure 3.4. Crack is a common problem for this kind of production techniques because of the unsatisfied lamination of the laminae.

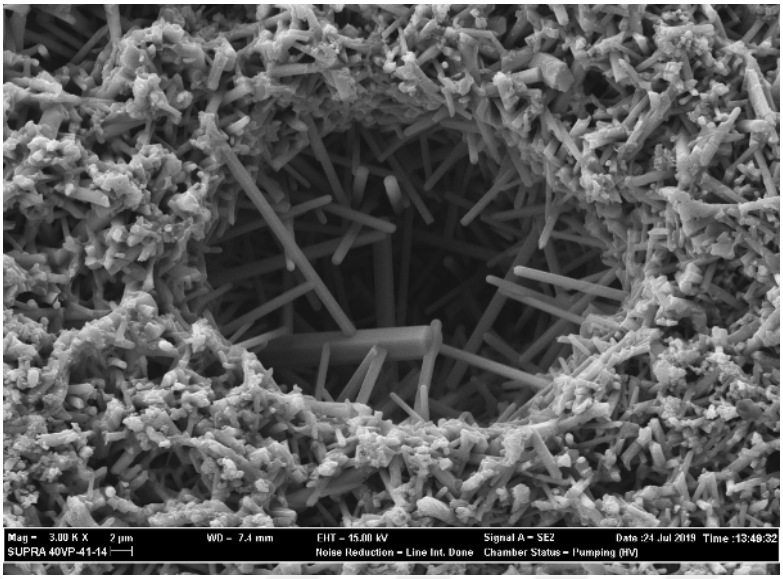

Figure 3.5 SEM image of porosity on the surface of Si_3N_4

The rod-like β grains can be seen in the Figure 3.5. These β grains was formed by the transformation of unstable α grains to the more stable β grains at high temperatures. Also, α-Si_3N_4 grains are existed. This uncompleted transformation of α grains to β grains can be the reason of low sintering temperature and sintering time. The samples were produced by the α-Si_3N_4 as a starting powder and rod-like β grains were formed. These β grains were brought on the formation of the interconnected network structure in 3-dimension. The usage of α-Si_3N_4 as a starting powder causes to the formation of anisotropic β grains.

As seen in the Figure 3.5, the rod-like elongated β grains can be seen through the pores. The usage of α-Si_3N_4 accelerates the driving force for formation of β-Si_3N_4 and due to this acceleration β grains tend to grow to pores where grain energies are low.

These α structures were correlated with the XRD results. Also, the open pore structure on the surface of the samples can be seen in the Figure 3.5.

The elemental analysis of the samples was done by EDX. The EDX analysis was taken from the area which is shown in Figure 3.6.

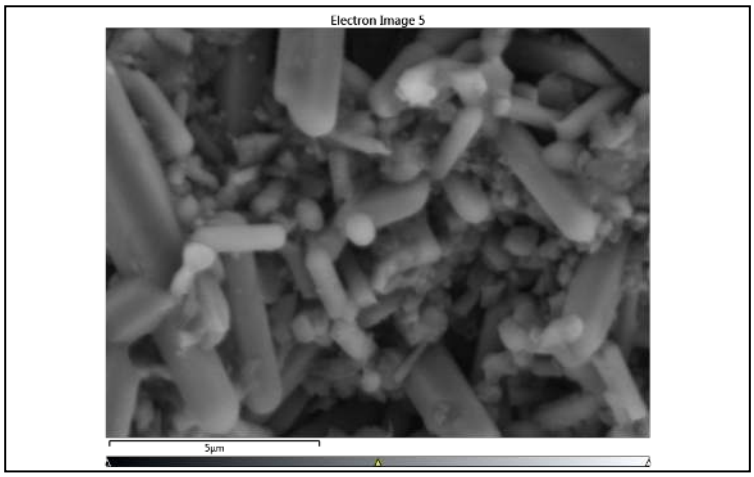

Figure 3.6 SEM figure of Si_3N_4 for EDX analysis

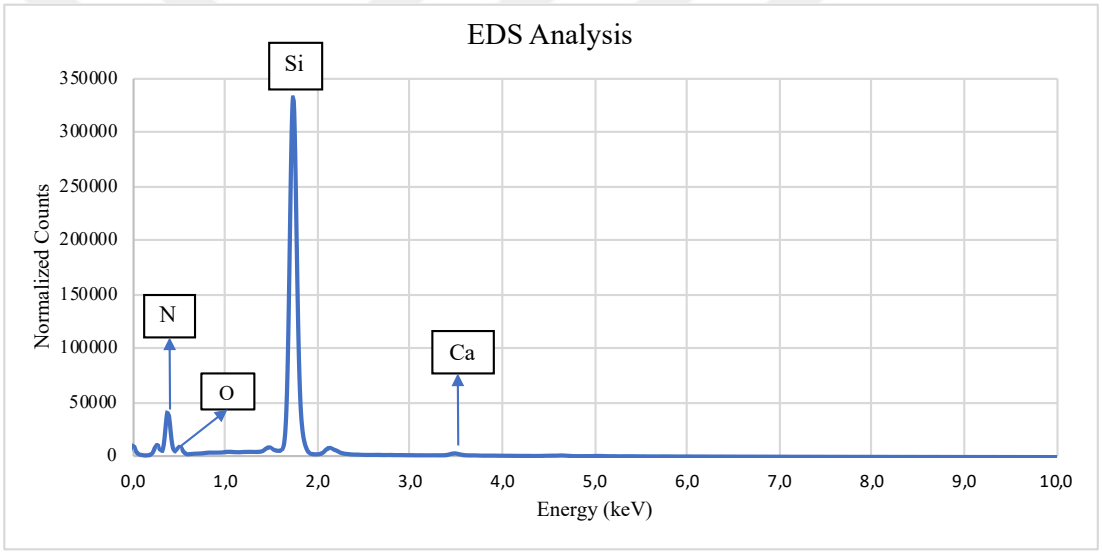

Figure 3.7 Elemental analysis of the samples

This analysis showed Si (55 wt.%) as the most common element which is followed by N (29.5 wt.%), O (3.0 wt. %) and Ca (0.2 wt.%). Ca and O were the sintering additives.

3.3. Cell Culture Tests

3.3.1. Cell Proliferation on Gradient Porous Si_3N_4 Ceramics

Cell proliferation analysis was done for gradient porous Si_3N_4 samples on days 3, 7 and 10. The absorbance value at 440 nm is the value for the yellow colored formazan product. WST-1 results suggest that cells seeded on scaffolds continue to increase in culture.

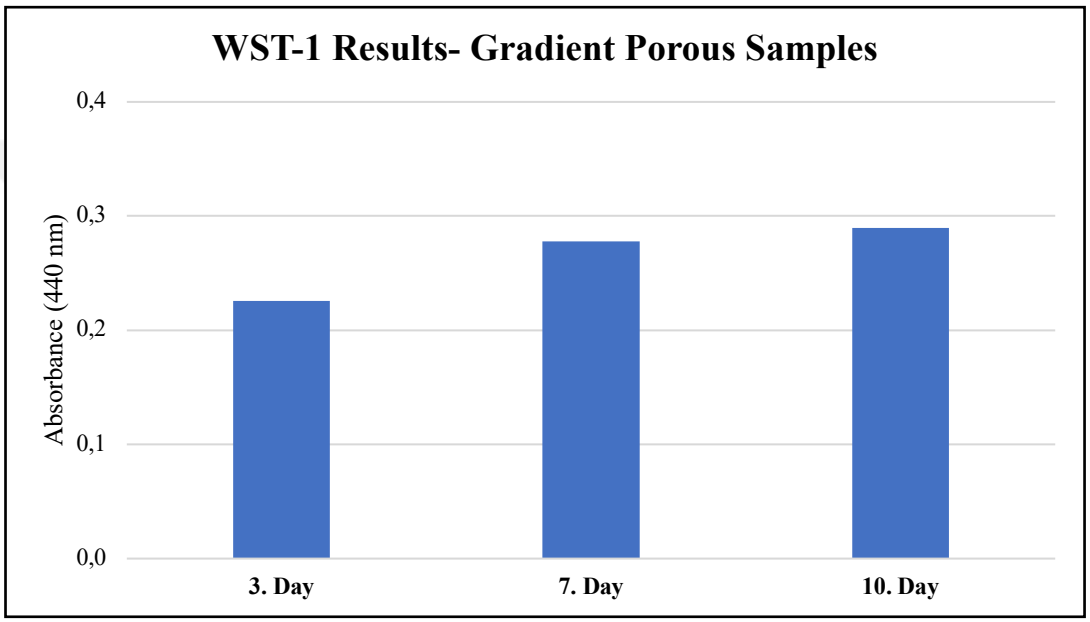

Figure 3.8 WST-1 absorbance graph of gradient porous sample.

3.3.2. Cytotoxic Analysis of Gradient Porous Si_3N_4 Ceramics

The cytotoxic evolution of the graded porous Si_3N_4 ceramics were done by lactate dehydrogenase activity of the cells. This technique is basically called as (LDH). The cytotoxic evaluation of gradient porous samples on days 3, 7 and 10. Readings were done at 492 nm after 60 mins. of incubation time according to manufacturer's protocole.

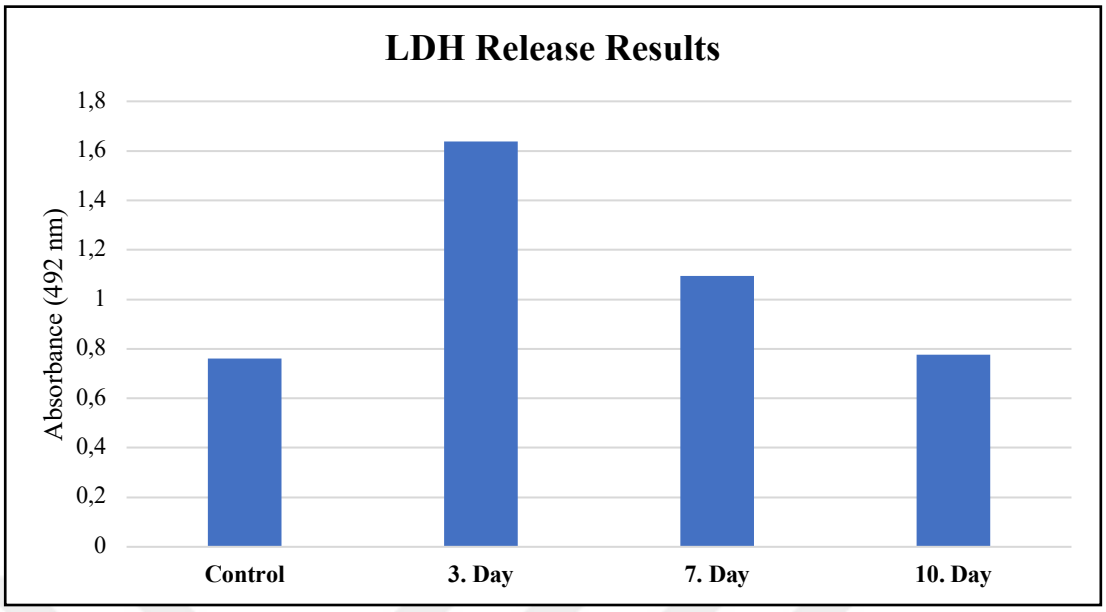

Figure 3.9 LDH absorbance values at 3. day, 7. day and 10. Day for gradient porous samples (measurements at 60 mins incubation).

As seen in Figure 3.9, absorbance values were similar as controls at day 10. This result is in correlation with the WST-1 results where cells proliferated, suggesting non-toxic behavior of the scaffolds.

3.3.3. Cell Adhesion on Gradient Porous Si_3N_4 Ceramics

DAPI stains the DNA and diffuses into the nuclei of the cells. The relationship between cell behavior and cell shape was mentioned in Figure 2.12.

Figure 3.10 is the image of 3rd day of the cell growth on the surface of the gradient porous samples.

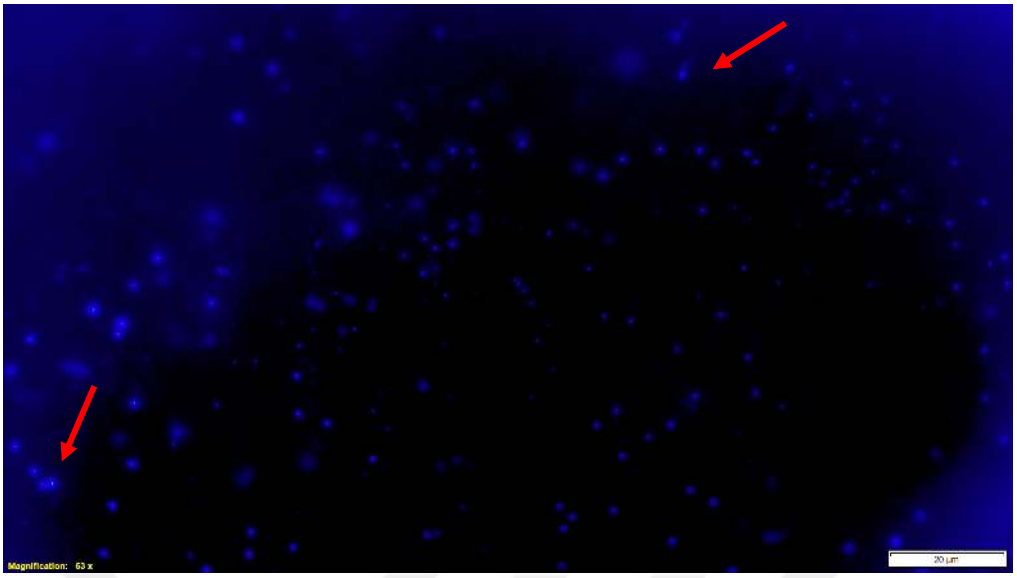

Figure 3.10 DAPI stained MG-63 cells at 3rd day (4x magnification)

As seen in the Figure 3.10, cells, at 3rd day, existed on the surface of the gradient porous samples and during proliferation of the some of the cells, fixation was done, and it was showed by red arrow.

Figure 3.11 is the 10x magnification where cells can be seen more clearly.

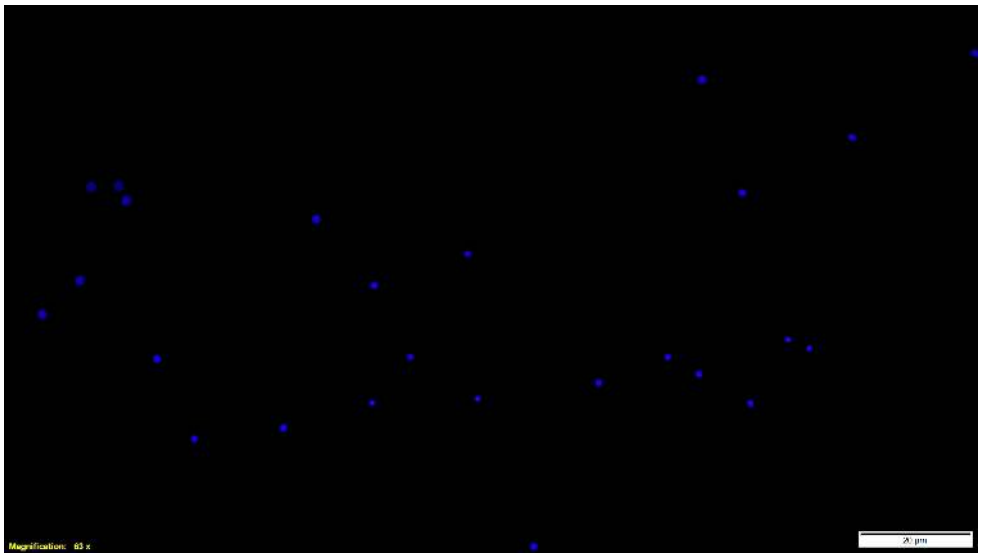

Figure 3.11 DAPI stained MG-63 cells at 3rd day (10x magnification)

Figure 3.11 is the visualization of the cells at 3rd day in the 10x magnification where the situation of the nucleus of the of the cells such as shape can be seen more clearly. Their shapes are rounded and regular.
Figure 3.12 is the cells on the surface of the samples at 20x magnification.

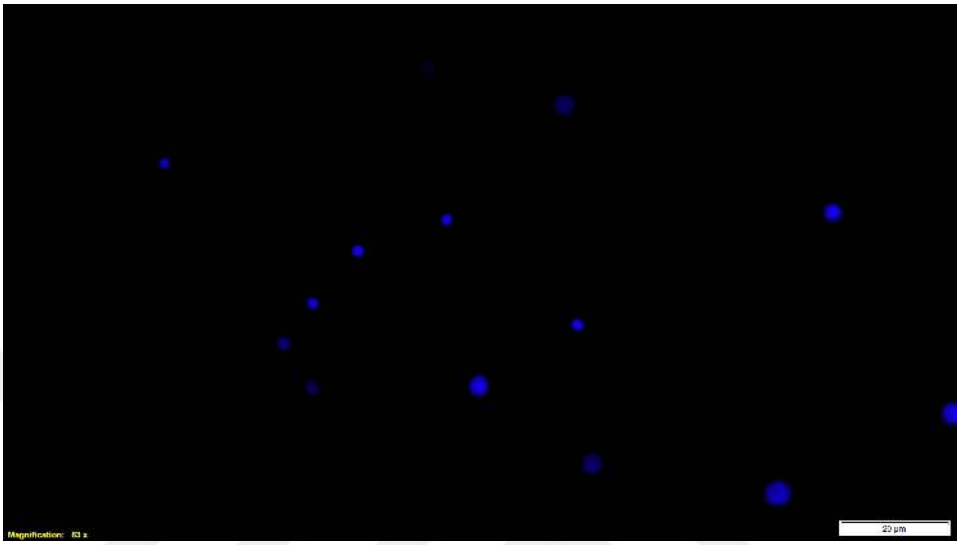

Figure 3.12 DAPI stained MG-63 cells at 3rd day (20x magnification)

The nucleus of the cells can be seen clearly where their shape was rounded and regular which is proof the healthy situation of the cells as seen on in Figure 3.12.

The fluorescent visualization of the MG-63 cells on the surface of gradient porous samples also was done at 7th day. Figure 3.13 is the 7th day image at 4x magnification.

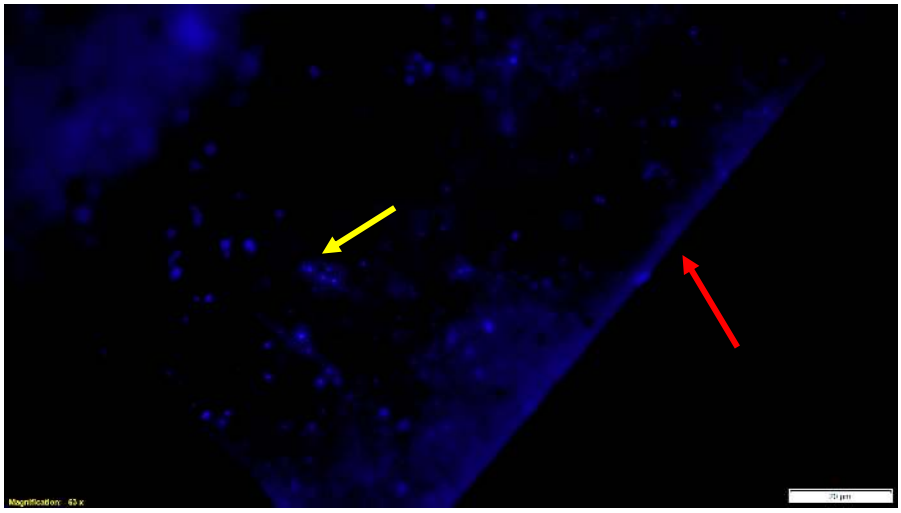

Figure 3.13 DAPI stained MG-63 cells at 7th day (4x magnification)

As seen in Figure 3.13, cells agglutinated which is showed by yellow arrow and this behavior of the cells cannot be seen normally but while they were on the surface of the foreign materials cells behaved but just some of them behave like this. Red arrow showed the edge of the samples.

In Figure 3.14, the cell on the edge of the pore can be seen and labelled with red arrow.

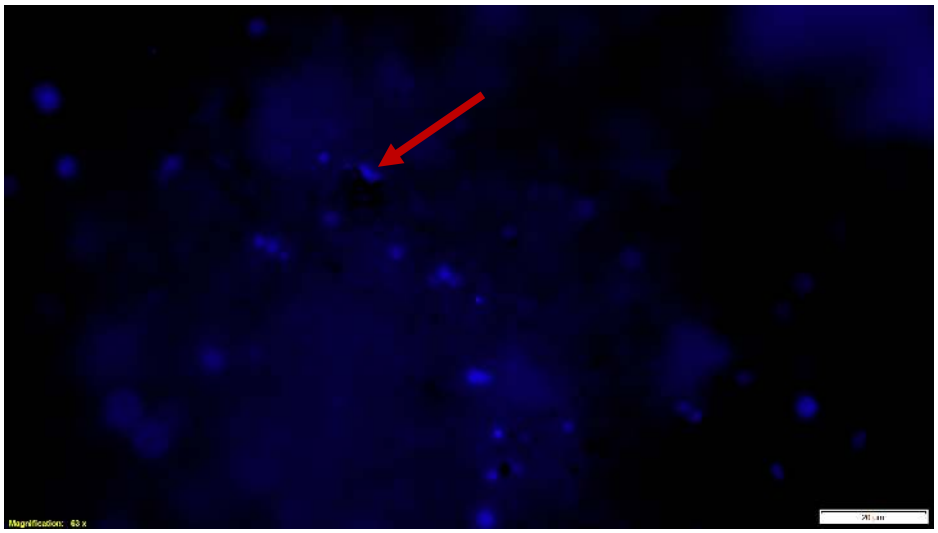

Figure 3.14 DAPI stained MG-63 cells at 7th day (4x magnification) and the cell on the edge of pore labelled with red arrow.

Cells can have a tendency to grow through the pore and pore was not show any negative effect to the cell which can be seen in Figure 3.14.

Figure 3.15 is the image at 10x magnification where some of the cells aggregate and Figure 3.16 is the image at 20x magnification of the similar cell aggregate.

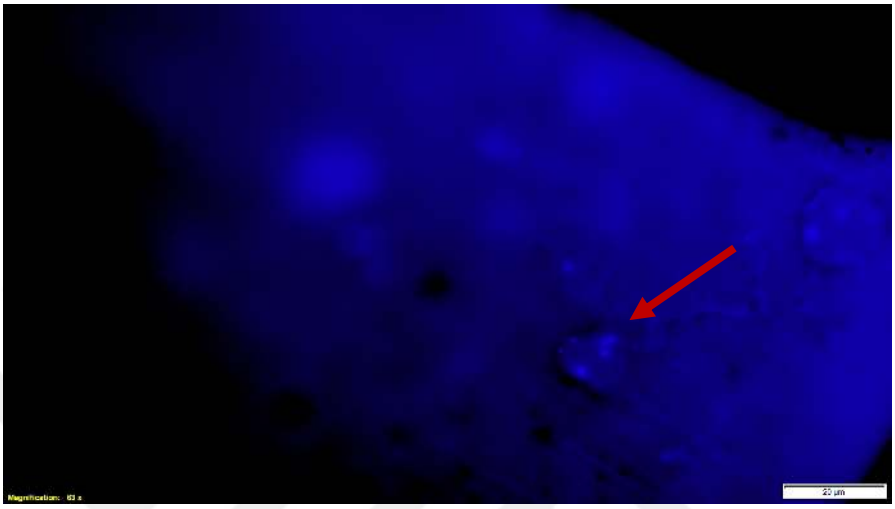

Figure 3.15 DAPI stained MG-63 cells at 7th day (10x magnification); red arrow shows the cell aggregation.

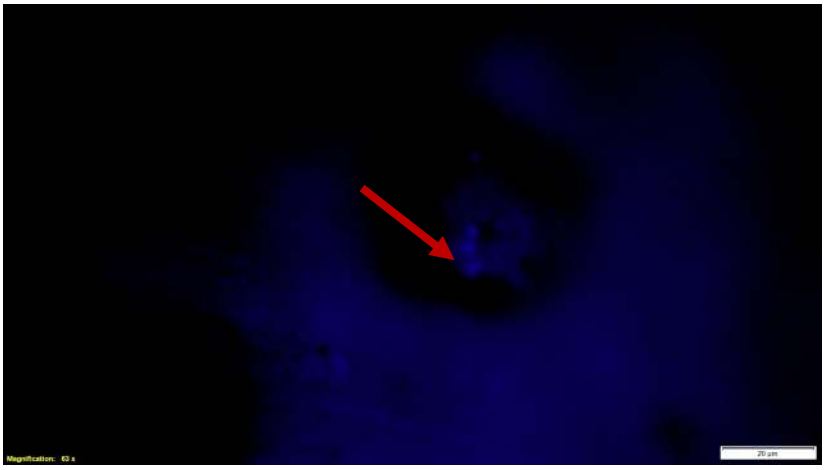

Figure 3.16 DAPI stained MG-63 cells at 7th day (20x magnification); red arrow shows the cell aggregation.

The nucleus of8 the cells also visualized by fluorescent microscope for the 10th day at the magnifications of 4x, 10x and 20x, respectively.

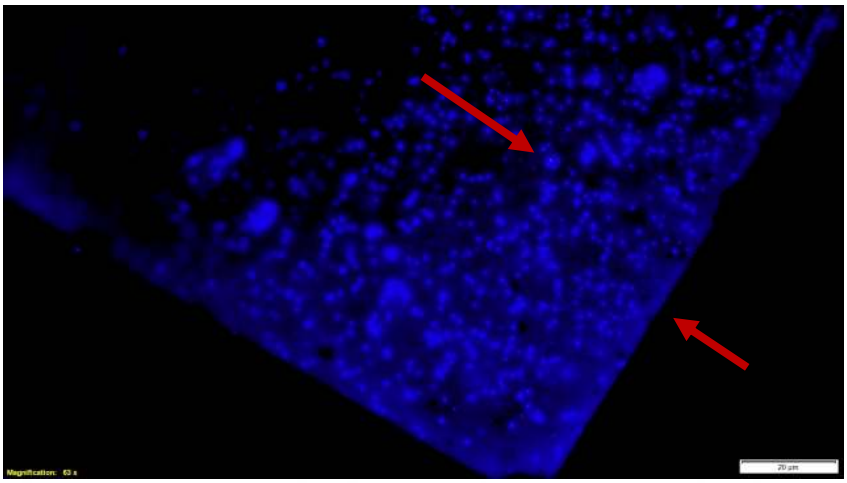

Figure 3.17 DAPI stained MG-63 cells at 10th day (4x magnification); red arrow shows the edge of the sample

At 10th day, number of cells increased which can be seen in the Figure 3.17. At the 10th day some of the cells continued aggregation which is showed in the Figure 3.17. The cell aggregation can be seen clearly in the Figure 3.18.

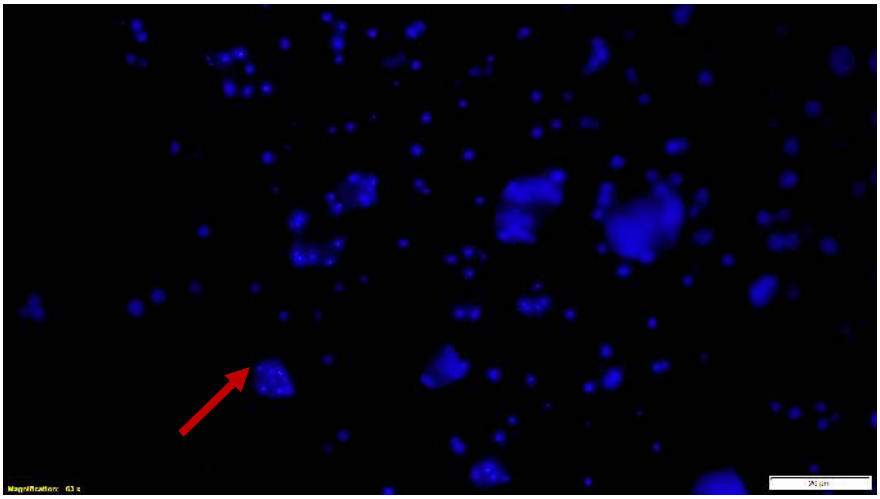

Figure 3.18 DAPI stained MG-63 cells at 10th day (10x magnification); red arrow shows the cell agglutination.

As seen in the Figure 3.18, beside the aggregation, cells proliferated, and they have rounded nucleus shape at the 10th day. This density of the cells supported with the WST-1 results and LDH results on the 10th day.

The 20x magnification of the image at 10th day can be seen in the Figure 3.19.

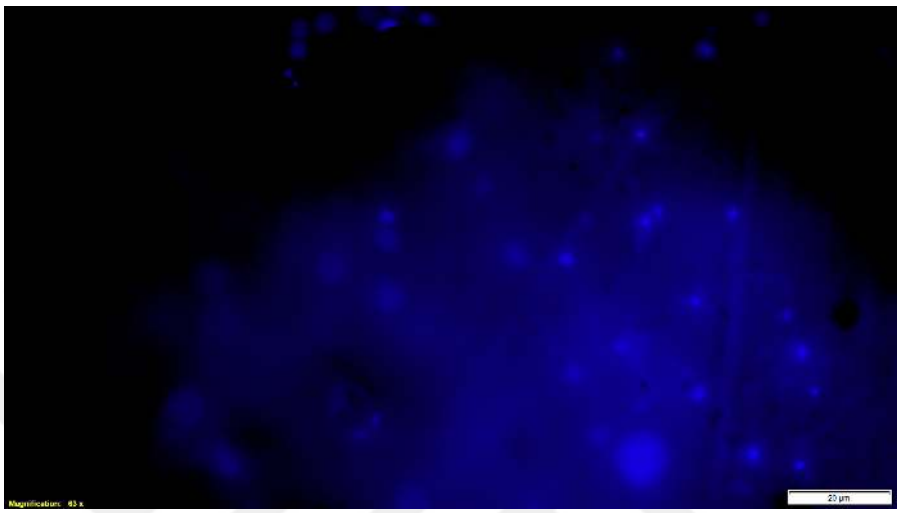

Figure 3.19 DAPI stained MG-63 cells at 10th day (20x magnification)

The rounded and regular shape of the nucleus of the cells can be seen clearly in the Figure of 3.19. Some of the cells were found inside of the pores which was shown in the Figure 3.20.

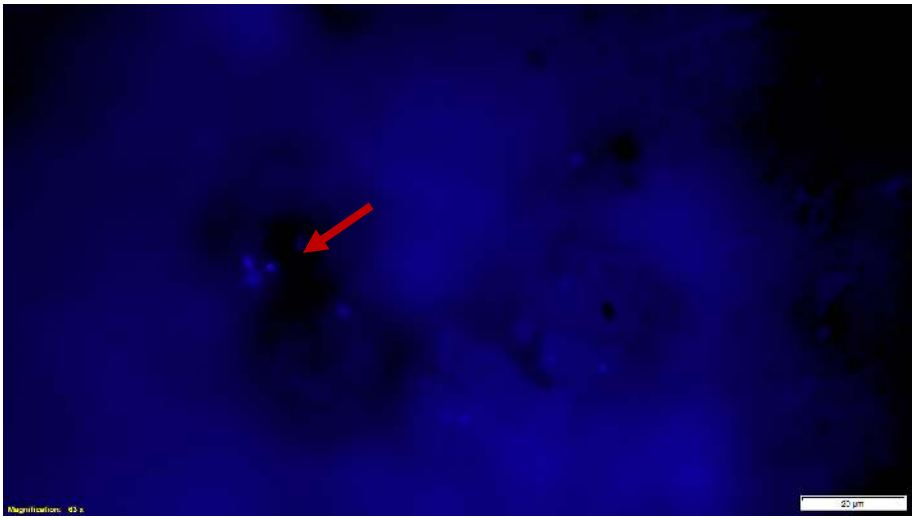

Figure 3.20. DAPI stained MG-63 cells at 10th day (20x magnification)

Cell was found inside of the pore that can be seen in the Figure 3.20 which is required behavior from cells, and which was compatible of the aim of this thesis.

As seen on both of the fluorescent images of the cells for all 3rd, 7th and 10th day, cells had a tendency to proliferation, and they have rounded and regular shape which were mentioned previously. This characteristics on the shape of the nucleus of the cells shows the how cells were healthy.

Zanocco et. al. discussed the proliferation of the osteoblast cells on the surface of Si_3N_4. In their study, the nuclei of the cells visualized by fluorescent microscopy where nuclei of the cells were stained by DAPI. The fluorescent microscopy micrograph of this study can be seen in Figure 3.21.

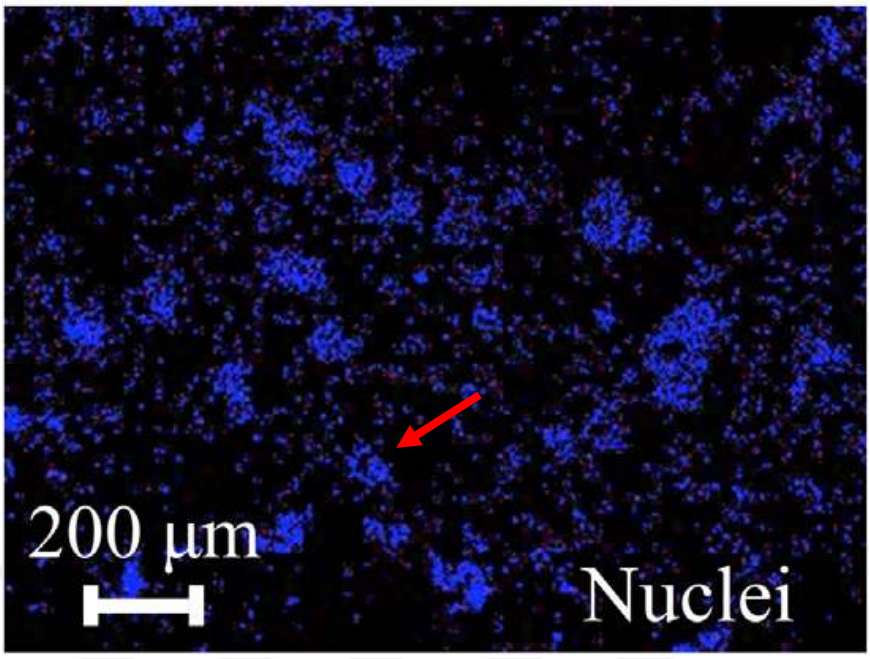

Figure 3.21 Fluorescent image of DAPI stained SAOS-2 Osteosarcoma cells on the Si_3N_4 [48].

The cell aggregation was observed also in this study which was shown by red arrow in the Figure 3.21.

Beside the visualization of the cells, as seen on both fluorescent microscope images, some of the regions were blur on the same image. The reason of this blur was the surface of the samples were not flat because of the occurred deformity during sintering.

For the better resolution on the fluorescent microscopy, the flat sample surface was required.

CHAPTER 4

CONCLUSION

In this study, gradient porous samples were produced, and they were characterized in means of physical, microstructural, phase and biocompatibility.

The lower bulk density value for gradient porous samples (1.63 g/cm^3) was obtained as a result of using limited amount of sintering additive and lower sintering temperature. Gradient structure was formed by using two types of pore former additives with different sizes and shapes.

Phase analysis showed that the presences of β-Si_3N_4 as the major phase and α-Si_3N_4 as the minor phase owing to restricted amount of sintering additives and low sintering temperature. SEM images of gradient sample from the cross-section showed the targeted pore characteristic was successfully formed; the amount and size of pores increased from bottom to top along the cross-section. SEM studies of samples showed that both forms of Si_3N_4 were existed in the samples. Equiaxed, spherical grains belonged to α-Si_3N_4 where β-Si_3N_4 had elongated, fiber-like morphology. The EDX study also proved the entity of Si_3N_4.

The biocompatibility was analyzed by two different tests, (1) is WST-1 is used to test cell activity and proliferation. The increase (in the metabolic substances and enzymes in the cell culture medium) reflect the increase in cell number. Cells proliferate on the surface of the samples suggesting that sample has no toxic effect. This cell proliferation is also proof of osseointegration where there is connection between cell and sample interface and cell attached on the surface of samples.

The cytotoxic evolution of the samples was analyzed by lactate dehydrogenase tests. Test results suggested that gradient porous Si_3N_4 samples had no toxic effect on the human osteoblast cells.

The fluorescent visualization of the nucleus of the cells on the surface of gradient porous Si_3N_4 samples showed that, cells attached to surface and continue to proliferate.

Besides that, as seen on figures, some cells growth in the pores. The rounded and regular shape of the cells proved that, cells were healthy, and they had a potential to proliferate. The histological analysis supported with the cytotoxic and proliferation analysis.

In conclusion, our data suggest that gradient porous Si_3N_4 ceramics may be possible candidates to be as bone substitute elements.

FUTURE STUDIES

- Producing the samples with interconnected porous structure
- Increasing the pore sizes
- Mechanical characterization of the samples
- Choosing different sintering aids
- Adjusting of the sintering conditions
- Staining with the different fluorescent dye
- SEM image of the cells on the surface of the samples

REFERENCES

[1] Studart, A., R., Gonzenbach U., T., Tervoort, E., and Gauckler, L., J., Gauckler, "Processing routes to macroporous ceramics: A review," J. Am. Ceram. Soc., 89 (6), 1771–1789, 2006.

[2] Miao, X., and Sun, D., "Graded/gradient porous biomaterials," Materials (Basel)., 3 (1), 26–47, 2010.

[3] Dorozhkin, S., V., "Bioceramics of calcium orthophosphates," Biomaterials, 31 (7), 1465–1485, 2010.

[4] Ryan, G., Pandit, A., and Apatsidis, D., P., "Fabrication methods of porous metals for use in orthopaedic applications," Biomaterials, 27 (13), 2651–2670, 2006.

[5] Colombo, P., Vakifahmetoglu, C., and Costacurta, S., "Fabrication of ceramic components with hierarchical porosity," J. Mater. Sci., 45 (20), 5425–5455, 2010.

[6] Rahaman, M., N., *"Ceramic Processing and Sintering"*, 2nd ed., Marcel Dekker Inc. New York, 2003.

[7] Nishihora, R., K., Rachadel, P., L., Quadri, M., G., N., and Hotza, D., "Manufacturing porous ceramic materials by tape casting—A review," J. Eur. Ceram. Soc., 38 (4) 988–1001, 2018.

[8] Colombo, P., "Conventional and novel processing methods for cellular ceramics," Philos. Trans. R. Soc. A Math. Phys. Eng. Sci., 364, (1838), 109–124, 2006.

[9] Kim, C., S., Randow, C., and Sano, T., "Hybrid and hierarchical composite materials" no. April. 2015.

[10] Walden, M., Bone Structure Retrieved October 3, 2019 from https://www.teachpe.com/anatomy-physiology/structure-of-bones

[11] Simancik, F., Reproducibility of Aluminium Foam Properties, Retrieved September 29, 2019 from https://www.researchgate.net/figure/Non-uniform-gradient-cellular-structures-a-natural-structure-of-bone-b-artificial_fig1_237534745

[12] Lee, S., et al., "Potential bone replacement materials prepared by two methods," Mater. Res. Soc. Symp. Proc., 1418, 177–188, 2012.

[13] Campana, V., et al., "Bone substitutes in orthopaedic surgery: from basic science to clinical practice," J. Mater. Sci. Mater. Med., 25, (10) 2445–2461, 2014.

[14] Jabbari, M., Bulatova, R., Tok, A., I., Y., Bahl, C., R., H., Mitsoulis, E., and Hattel, J., H., "Ceramic tape casting: A review of current methods and trends with emphasis on rheological behaviour and flow analysis," Mater. Sci. Eng. B Solid-State Mater. Adv. Technol., 212, 39–61, 2016.

[15] Kao, S., T., and Scott, D., D., "A Review of Bone Substitutes," Oral Maxillofac. Surg. Clin. North Am., 19 (4), 513–521, 2007.

[16] Lingala, S., M., and Mhs, M., G., Ghany, M., "Bone Mechanical Properties in Healthy and Diseased States" HHS Public Access, 25, (3), pp. 289–313, 2016.

[17] Pezzotti, G., Marin, E., Adachi, T., Rondinella, A., Boschetto, F., Zhu, W., Sugano, N., Bock, R., M., and Bal, S., B., "Bioactive silicon nitride: A new therapeutic material for osteoarthropathy" Scientific Reports, 7(March), 1–11. https://doi.org/10.1038/srep44848

[18] Hoffmann, M., J., and Petzow, G., "Tailored microstructures of silicon nitride ceramics," Pure Appl. Chem., 66 (9), 1807–1814, 1994.

[19] Hoffmann, M., J., "Si3N4-Ceramics, Structure and Properties of," Ref. Modul. Mater. Sci. Mater. Eng., no. 10–13, 2016.

[20] High Purity Silicon Nitride Powder Retrieved August 3, 2019 from https://www.ube.com/contents/en/chemical/ceramics/ceramics.html

[21] Wang, L., Tien, T., and Chen, I., "Formation of beta-Silicon Nitride Crystals from (Si, Al, Mg, Y) (O, N) Liquid: I, Phase, Composition and Shape Evolutions" 91 (9) 1586–1591, 2003.

[22] Crystal Structures of Si_3N_4 Retrieved August 3, 2019 from http://www.hardmaterials.de/html/alpha-si3n4__beta-si3n4.html

[23] Sohrabi, A., Holland, C., Kue, R., Nagle, D., Hungerford, D., S., and Frondoza, C., G., "Proinflammatory cytokine expression of IL-1β and TNF-α by human osteoblast-like MG-63 cells upon exposure to silicon nitride in vitro," J. Biomed. Mater. Res., 50 (1), 43–49, 2000.

[24] Howlett, C., R., McCartney E., and Ching, W., "The Effect of Silicon Nitride Ceramic on Rabbit Skeletal Cells and Tissue," Clin. Orthop. Relat. Res., vol. NA; (244), 293-304, 2006.

[25] Ma, L., Song, Y., Li, X., Li, R.,Shang, Z.,Wang, Y., Guedes e Silva, C., C., Higa, O., Z., Bressiani, J., C., Pezzotti, G., Oba, N., Zhu, W., Marin, E., Rondinella, A., Boschetto, F., McEntire, B., Yamamoto, K., Bal, B. S. "Fabrication and properties of Si3N4 bioscaffolds with orderly–interconnected big pore channels and well–distributed small pores," Mater. Sci. Eng. C, 64, (10), 11730–11736, 2004.

[26] Neumann, A., Reske, T., Held, M., Jahnke, K., Ragoß, C., and Maier, H., R., "Comparative investigation of the biocompatibility of various silicon nitride ceramic qualities in vitro," J. Mater. Sci. Mater. Med., 15 (10), 1135–1140, 2004.

[27] Cecilia, J., C., Guedes e Silva, B., Bruno Ko¨nig, Jr., C., Carbonari, M., J., Yoshimoto, M., Allegrini, Jr., S., "Tissue response around silicon nitride implants in rabbits," J. Biomed. Mater. Res. A, 79 (4), 989–998, 2006.

[28] Mazzocchi, M., and Bellosi, A., "On the possibility of silicon nitride as a ceramic for structural orthopaedic implants. Part I: processing, microstructure, mechanical properties, cytotoxicity," J. Mater. Sci. Mater. Med., 19 (8), 2881–2887, 2008.

[29] Bal, B., S., and Rahaman, M., N., "Orthopedic applications of silicon nitride ceramics," Acta Biomater., 8 (8), pp. 2889–2898, 2012.

[30] Youssef, J., A., Myhre, S., L., and Bal, B., S., "Musculoskeletal Disorders and Treatment Radiographic Follow-up of Transforaminal Lumbar Fusion with Silicon Nitride Spacers: A case Report of Two Patients ClinMed International Library," J. Musculoskelet. Disord. Treat., 2 (1), pp. 1–8, 2016.

[31] Pezzotti, G., Bock, R., M., Adachi, T., Rondinella, A., Boschetto, F., Zhu, W., Marin, E., McEntire, B., Bal, B., S.,Mazda, O. "Silicon nitride surface chemistry: A potent regulator of mesenchymal progenitor cell activity in bone formation," Appl. Mater. Today, 9, 82–95, 2017.

[32] Ishikawa, M., de Mesy Bentley, K., L., McEntire, B., J., Bal, B., S., Schwarz, E., M., and Xie, C., "Surface topography of silicon nitride affects antimicrobial and osseointegrative properties of tibial implants in a murine model," J. Biomed. Mater. Res. - Part A, 105 (12), 3413–3421, 2017.

[33] Ohji, T., "Microstructural design and mechanical properties of porous silicon nitride ceramics," Mater. Sci. Eng. A, 498, (1–2), 5–11, 2008.

[34] Seeber, B., S., M., Gonzenbach, U., T., and Gauckler, L., J., "Mechanical properties of highly porous alumina foams," J. Mater. Res., 28 (17), 2281–2287, 2013.

[35] Twiname, E. R., & Mistler, R. E. (2001). Tape Casting and Lamination. Encyclopedia of Materials: Science and Technology, 1952(Howatt 1952), 9083–9088. https://doi.org/10.1016/b0-08-043152-6/01639-9

[36] Micromeritics Instrument Corporation,Mercury Porsimetry Intrusion Theory, Retrieved August 5, 2019 from https://www.micromeritics.com/Repository/Files/Mercury_Porosemitry_Theory_poster_.pdf

[37] Riss, T., L., Moravec, R., Niles, A., Duellman, S., Benink, H., A., and Worzella, T., J., Minor, L., "Cell Viability Assays," Assay Guid. Man., no. Md, 1–25, 2004.

[38] Thoma cell counting chamber, Retrieved August 5, 2019 from http://insilico.ehu.eus/counting_chamber/thoma.php

[39] Multi-well tissue culture plates, Retrieved August 5, 2019 from http://www.cellsignet.com/media/templ.html

[40] Kumar, P., Nagarajan, A., and Uchil, P., D., "Analysis of cell viability by the lactate dehydrogenase assay," Cold Spring Harb. Protoc., 6, 465–468, 2018.

[41] Khalili, A., A., and Ahmad, M., R., "A Review of cell adhesion studies for biomedical and biological applications," Int. J. Mol. Sci., 16 (8), 18149–18184, 2015.

[42] Kalemtas, A., Topates, G., Özcoban, H., Mandal, H., Kara, F., and Janssen, R., "Mechanical characterization of highly porous β-Si3N4 ceramics fabricated via partial sintering & starch addition," J. Eur. Ceram. Soc., (33) (9), 1507–1515, 2013.

[43] Yasemin Tabak, "Production of silicon nitride-based biomaterials by tape casting method for artifical bone applications and their characterization", Ph.D. Thesis, Kocaeli University, 2018.

[44] Bitterlich, B., and Heinrich, J., G., "Aqueous tape casting of silicon nitride," J. Eur. Ceram. Soc., (22), (13), 2427–2434, 2002.

[45] Bačáková, L. Filová, E., Rypáček, F., Švorčík, V., and Starý, V., "Cell Adhesion on Artificial Materials for Tissue Engineering," Physiol. Res., 53 (SUPPL 1), 2004.

[46] Jeewandara, T., Biomimetic Engineering: Learning From Future October 22, 2019, Retrieved December 5, 2019 from https://www.laboratory-journal.com/science/material-science/biomimetic-engineering-learning-nature

[47] Thielen, M., Extreme Biomimetics- the search for natural sources of materials engineering inspiration, May 2013, 23 Retrieved December 5, 2019 from https://phys.org/news/2019-10-extreme-biomimetics-natural-sources-materials.html

[48] Zanocco, M., Boschetto, F., Zhu, W., Marin, E., McEntire, B., J., Bal, B., S., Adachi, T., Yamamoto, T., Kanamura, N., Ohgitani, E., Yamamoto, K., Mazda, O., Pezzotti, G. "3D-additive deposition of an antibacterial and osteogenic silicon nitride coating on orthopaedic titanium substrate," J. Mech. Behav. Biomed. Mater., 103, 103557, 2020.

[49] Zhu, X., and Sakka, Y., "Textured silicon nitride: Processing and anisotropic properties," Sci. Technol. Adv. Mater., 9 (3), 2008.

CIRRICULUM VITAE

PERSONAL INFORMATION

Name Surname: Serdar Onat AKBULUT

Date of Birth: 02.11.1994

E-Mail: serdaronatakbulut@hotmail.com

RESERCH INTEREST

- Porous Ceramics
- Ceramics and Non-Oxide Ceramics
- Tape Casting
- Tissue Engineering
- Bone Tissue
- Bone Grafts and Substitutes
- Cell Culture
- Biocompatibility
- Biomimicking

EDUCATION

2018-2020 **Ankara Yıldırım Beyazıt University**

M.Sc., Materials Engineering

Thesis: "Production of Gradient Porous Si_3N_4 Ceramics for Bone Grafting Applications"

2012-2018 **Ankara Yıldırım Beyazıt University**

B.Sc., Metallurgical and Materials Engineering

Graduation Project: "Biocompatibility of Porous Si_3N_4 Based Ceramics

INTERNSHIPS

June-August 2016 **Nurol Technology Inc.**

June-August 2015 **Kaptan Iron-Steel Inc.**

PROJECTS

- Researching of Biocompatibility of Gradient Porous Si_3N_4 Ceramics with Living Cell Analysis, Researcher (2019), AYBU Scientific Research Projects (5363)

CONFERENCE PRESENTATIONS and ABSTRACTS

- Üstünçelik, M., Özkahya, B., Akbulut, S., O., Topateş, G., "Production and Characterization of Silicon Nitride Ceramics with Graded Pore Structure" 3rd International Porous and Powder Materials Symposium and Exhibition, 90, 12-15 September 2017, Turkey. (Abstract, Oral Presenation)

- Akbulut, S., O., Üstünçelik, M., "Biocompatibility of Si_3N_4 Ceramics" 6. National Bioengineering Student Congress, 27, 5-6 April 2018, Turkey. (Abstract, Oral Presentation)

- Akbulut, S., O., Ozbek, B., İ., Butterworth, A., Ghorbanpoor, H., Avcıoglu, G., Akbaş, Y., Oksuz, S., Kozaci, L., D., Topateş, G., Guzel, F., D., Corrigan, D., Avci, H., "Novel Nanofibre Integrated SiN Scaffolds for Skeletal Implant Applications" 14th Nanoscience and Nanotechnology Conference, 163, 22-25 September 2018, Turkey. (Abstarct, Oral Presentation)

- Akbulut, S., O., Ozbek, B., I., Butterworth, A., Ghorbanpoor, H., Avcıoglu, G., Kozacı, L., D., Topateş, G., Corrigan, D., Avcı, H., Güzel, F., D., "Impedance Testing of Porous Si_3N_4 Scaffolds for Skeletal Implant Application", 5th International Conferences on Engineering Sciences, 60, 19 September 2019, Turkey. (Abstract, Oral Presenation)

REFERENCES

- Assist. Dr. Gülsüm TOPATEŞ, Ankara Yildirim Beyazit University, Metallurgical and Materials Engineering, gtopates@ybu.edu.tr

- Prof. Dr. Cihangir DURAN, Ankara Yildirim Beyazit University, Metallurgical and Materials Engineering, cihangirduran@yahoo.com

- Prof. Dr. Leyla Didem KOZACI, Ankara Yildirim Beyazit University, Faculty of Medicine, Medical Biochemistry, ldkozaci@yahoo.com

- Assist. Dr. Fatma DOĞAN GÜZEL, Ankara Yildirim Beyazit University, Biomedical Engineering, fdogan@ybu.edu.tr